GROUND AND FLIGHT TEST PROGRAM OF A STOKES-FLOW PARACHUTE

PACKAGING, DEPLOYMENT, AND SOUNDING ROCKET INTEGRATION

FINAL REPORT ON CONTRACT NAS1-10947

NASA CR-112251

P. G. Niederer and D. J. Mihora

September 27, 1972

Prepared by

ASTRO RESEARCH CORPORATION
Santa Barbara, California

for

NATIONAL AERONAUTICS AND SPACE ADMINISTRATION
LANGLEY RESEARCH CENTER

SUMMARY

The work reported here was performed in support of a NASA Langley Research Center program which called for the development of a Stokes-flow parachute, which, as a sonde, would obtain high altitude, meteorological data. The principal part of the investigation was the development of means of inflating the parachute braces and packaging the assembly. This report describes in detail the current design and hardware components of the patented 14 m^2 Stokes-flow parachute. The investigation concluded with an evaluation of data obtained from NASA's four, high altitude, flight tests of the parachute.

The Stokes-flow parachute is a canopy of open mesh material, which is kept deployed by braces. Because of the light weight of its mesh material, and the high drag on its mesh elements when they operate in the Stokes-flow flight regime, this parachute can have an extremely low ballistic coefficient. It provides a stable aerodynamic platform superior to conventional nonporous billowed parachutes, is exceptionally packable, and is easily contained within the canister of the Sidewinder Arcas or the RDT & E rockets. Thus, it offers the potential for gathering more meteorological data, especially at high altitudes, than conventional billowed parachutes.

For the present application a 14 m^2 canopy was developed which was calculated to have a ballistic coefficient of 0.02 kg/m^2 when operated as a winddrifter, or a coefficient of 0.04 kg/m^2 when supporting a radio sonde of 0.175 kg. The deployment braces are two, center-manifolded, inflatable tubes made of two mil Mylar. Part of the investigation was to develop means for automatically inflating these tubular braces when the packaged parachute is released above 80 km from a rocket-launched canister. The selected pressurizing fluid was n-pentane; 3.3 grams are required to properly inflate each of the four brace legs. Methods are recommended for encapsulating the n-pentane while the parachute is packaged, and for releasing it for brace inflation.

Methods for packaging the parachute are also recommended. These methods include schemes for folding the canopy and for automatically releasing the pressurizing fluid as the packaged parachute unfolds.

Evaluation of the four flight tests, the first in a series

of tests that will be performed, showed that the braces of the parachutes were unable to deploy the canopies. This was due to deployment being initiated, for all four tests, at altitudes and velocities whose dynamic pressures were greater than the design capability of the braces. It is recommended that future flight tests be initiated in dynamic pressure regimes within the deployment capability of the present brace design. Otherwise, the brace design can be strengthened so that they can deploy the canopies in harsher flight regimes.

CONTENTS

ILLUSTRATIONS

INTRODUCTION

The determination of atmospheric conditions at altitudes from 30 to 100 km is presently accomplished by relatively small, expendable sounding-rocket systems. These usually consist of a carrier rocket, an instrumented radiosonde that is ejected near the rocket's apogee, and a parachute.

The quality of high-altitude soundings depends to a large extent on the capabilities of the parachute of the system. Its most important purpose is to assure the lowest possible descent velocity of the radiosonde, so that vertical resolution of data is maximized. Measurements of temperature generally require that the sonde operate at subsonic velocities. Strong vibrations and violent oscillations are detrimental to the smooth operation of the instruments, and may cause vastly increased noise levels and output errors. The parachute, therefore, should provide an aerodynamically stable descent, without coning motions or gliding tendencies, if the system is to serve as a wind sensor.

Operational requirements reflect the severity of environmental conditions to which the parachute is exposed. They include tight packability into the rocket vehicle and reliable, fully-automatic deployment instantly after explosive ejection from the rocket which may be spinning at 15 cycles per second. The parachute should, in addition, be radar reflective for ground-tracking purposes. Its partial or total collapse below 20 to 30 km is desirable to reduce inordinately long dwelling times at these altitudes. Being part of an expendable system, the parachute should be inexpensive, and suitable for large-scale manufacture and easy handling.

The Stokes-flow decelerator (Ref. 1) is an extremely lightweight aerodynamic drag device. Its design takes advantage of minimum gauge filaments that are used to form a finely textured open-mesh canopy of high drag-producing efficiency because of viscous flow effects.

The immediate purpose of the development of the Stokes-flow decelerator is to improve the quality of high-altitude data sampling, by providing an aerodynamically stable parachute which descends more slowly than parachutes now in operational use. The target performance presently considered is to achieve subsonic descent of a radiosonde of 0.175 kg mass from an altitude of at least 80 km.

The development of the Stokes-flow decelerator through several stages has been reported in detail in References 2, 3, 4, and 5. A theory of the aerodynamic drag of open-mesh canopies in viscous flow, and two early structural concepts of the square X-brace parachute and the circular toroid parachute are described in References 2 and 3. The designs of these parachutes for Dart and Arcas missions include nine suspension lines to support rather heavy payloads. With the current trend toward significantly more lightweight payloads in the 0.1 to 0.2 kg range, parachute designs could be simplified, for example, by reducing the number of suspension lines to a single central line. Several single-line concepts have subsequently been studied, subjected to optimization procedures, and drop tested to evaluate structural integrity, as reported extensively in References 4 and 5.

This report describes the activities preliminary to and including a first series of full-scale rocket flight tests of experimental Stokes-flow parachutes. The selection of an X-brace parachute with inflatable tubular braces and with a single, central suspension line has been recommended in Reference 5 (Concept 1) as the most promising candidate for immediate further development and testing. This selection has been based on the following significant advantages:

- Ease of fabrication and packaging
- Capability of operation either as a winddrifter or as a payload-carrying device
- Flexibility of design
- High drag-producing efficiency
- Anticipated excellent aerodynamic stability.

A comparison of expected performance of the 14 m^2 X-brace parachute with other high-altitude drag devices is shown in Table II of Reference 5. A ballistic coefficient of less than 0.04 kg/m^2 for the parachute with a payload of 0.175 kg is from two to six times lower than that of other payload-carrying parachutes. When the parachute is used as a winddrifter, ballistic coefficient is further reduced to less than 0.02 kg/m^2. Since the present target performance of the system requires a ballistic coefficient of not more than 0.07 kg/m^2, the Stokes-flow parachute is expected to descend subsonically from well above 80 km if properly ejected from the rocket vehicle.

This report describes in detail the current design and hardware components of the Stokes-Flow parachute, including material listings and fabrication techniques. Also included is a discussion of the packaging and operating procedures.

. Parachute Engineering and Design Data

These data, extracted largely from Reference 5, are the bases for the design and fabrication of experimental parachutes and their associated hardware.

. Development of Inflation Capsules

The rapid, reliable, and fully automatic deployment of the parachute is dependent on the proper operation of a device that controls injection of the inflation substance into the braces. The all-soft inflation capsules developed for the Stokes-flow parachute are designed to release an amount of pentane within two to three seconds from parachute ejection, slowly enough to prevent explosive expansion of the braces. The development of these capsules is described, including their designs and results from limited environmental testing.

. Parachute Packaging and Deployment

Several packaging schemes for full-scale, X-brace parachutes are reviewed and evaluated for application to a canister of Arcas or RDT & E dimensions. The spiral-wrapping procedure is most desirable and has been developed through all phases of folding the parachute and its storage in a clam-shell container that fits into the rocket body. The spiral scheme has been tested successfully in a full-scale ejection and deployment test in the 40-ft sphere at NASA Langley Research Center.

. Full Scale Testing

Appendix D of this report is entitled "June, 1972, Wallops Island Flight Tests of the Stokes-Flow Parachute" and describes the following major topics:

1. Discussion of flight test data
2. Restated flight test guidelines
3. Recommendations/future applications

PARACHUTE ENGINEERING AND DESIGN DATA

The design of the experimental parachute considered for flight testing has been developed and analyzed in detail in Reference 5, Concept 1. The parachute is a square, X-brace design with tubular, inflatable braces and one central suspension line to carry a payload of 0.175 kg. Following is a list of more detailed characteristics:

1. Canopy

Projected area:	$A = 14\ m^2$
Canopy-rise angle:	25° (see Ref. 5)
Surface area:	$A' = 16.1\ m^2$
Material:	Mylar - nylon composite knit by Dow-Badische, type DD, solidity - $\epsilon = 0.19$, surface density - $m_1 = 5\ g/m^2$

2. Braces

Total length:	L = 5.29 m (each leg, Ll = 2.645 m)
Diameter:	d = 0.088 m
Material:	Mylar laminate type P2-5508.36 by Dow Chemical, thickness - $t = 1.65 \times 10^{-5}$ m (0.65 mil) 300 Å aluminum underneath 0.15 mil Mylar layer.

The four brace legs are attached to a pressure manifold, Langley Research Center design, placed at the center of the canopy, as shown in Figure 1. The braces are attached to the canopy along continuous lines. In the present configuration, the braces are located below the canopy. Brace position above canopy may be considered in the future if flight tests indicate insufficient pressurization of the braces in the shadow of the canopy.

After its ejection from the rocket vehicle, the parachute is pressurized by controlled injection of n-pentane, Freon, or other volatile liquid stored in and released simultaneously from four

inflation capsules placed near the brace tips. A detailed description of design and development of the inflation capsules is given below. Reference 5 contains a discussion of the technical aspects of brace inflation. The amount of liquid required for full pressurization of the experimental parachutes is based on the following considerations.

The system is assumed to withstand full deployment with a load factor of 1.6 g immediately after ejection at 80 km altitude. Because of evaporation and expansion of the n-pentane, there is a phase of adiabatic cooling from an initial temperature of 300° K (sea level ambient) to 250° K, if the temperatures of the braces and the n-pentane are assumed equal. This implies a transfer of thermal energy of the braces into the inflation substance, as discussed in Reference 5 (also, see Fig. 45 of Ref. 5). Under these conditions, a total amount of 13.5 grams, or 21.2 cc of n-pentane is required for inflation.

After this initial phase of cooling of the braces, their temperature increases toward a state of equilibrium based on an exchange of thermal energy by radiation from the sun, the earth (IR albedo), and of the braces themselves. The solar absorptivity, α , and the emissivity, ϵ , of the braces with the aluminized layer (300 Å) toward the outside but underneath a layer of 0.15 mil of clear Mylar, has been determined experimentally by NASA-LRC:

$$\alpha = 0.149$$

$$\epsilon = 0.340$$

With a ratio of $\alpha/\epsilon = 0.438$, the temperature of thermal equilibrium of the braces at 80 km altitude above the earth is approximately 293° K (sun position at right angles to brace axis). The resulting levels of brace pressure (at negligible external pressure) and brace hoop stress are:

Condition	p(torr)	$\sigma(N/m^2)$
Load carrying at deployment (n = 1.6 g , T = 250° K)	45	16×10^6
Thermal equilibrium (n = 1 g , T = 293° K)	53	19×10^6

3. Suspension Line

The suspension line consists of a simple harness assembly of Dacron ribbon that is strapped on the parachute prior to packaging. A line length of 2.8 m has been selected to separate the payload from the canopy by a length of at least one brace leg. A full description of the line and its fabrication is given in Appendix A.

4. Breakdown of Masses

The following breakdown represents typical masses only.

Canopy, m_c	0.081 kg
Braces, m_b	0.089 kg
Inflation substance, m_v (n-pentane)	0.014 kg
Suspension line, m_s	0.011 kg
Total decelerator, m_d	0.195 kg
Payload, mp	0.175 kg
Total system, m	0.370 kg

DEVELOPMENT OF INFLATION CAPSULES

The Problem

The need of a device that will provide controlled deployment of the braces by rapid inflation was recognized early in this program (Ref. 2). Storage of the inflation substance directly in the brace volume causes almost instant vaporization of all substance when exposed to near vacuum conditions, and at the levels of pressure required to carry payloads, explosive brace rupture usually cannot be avoided. The exact causes of rupture are only qualitatively recognized at this time, and they defy rigorous theoretical analysis. Some limited experimentation has been described in Reference 5, and some further testing has been performed during the present program. Uncontrolled dynamic inflation tests of small brace tubes (radius: 2 cm, length: 100 cm) indicated that the maximum pressure, p_d , the tubes are able to withstand during deployment should not be more than approximately 7 $\pm$ 1 percent of the static equilibrium pressure after deployment. Static measurements of radii of curvature of partially unrolled brace tubes furthermore reveal an area of stress concentration in the flattened portion of the tube near the end that unrolls. Radii of curvature in that area indicate levels of stress that may considerably exceed twice the level of hoop stress in the cylindrical portion.

Brace deployment should, therefore, be controlled by a device or mechanism that prevents full pressurization of the braces to more than 7 percent of static pressure until full deployment has occurred. This can be achieved by encapsulating the inflation substance within the braces and by time-controlled injection into the brace volume through an orifice. The maximum allowable rate of fluid ejection during deployment can be estimated by relating deployment pressure to deployment rate. It can be assumed that the work done by the expanding vapor is equal to the sum of the energies of package rotation and parachute expansion. This assumption can be formulated in the following equation:

$$4r \sqrt{\frac{\pi\, p_d}{m_c\, \ell}}\, t = \sqrt{2} + \log_e (1 + \sqrt{2})$$

where

r = brace-tube radius

p_d = pressure during deployment

m_c = mass of parachute

ℓ = length of brace leg

t = time to full deployment

For the parachute considered here, the minimum deployment time according to this formula is $t = 0.22$ second; a total time of 2.5 seconds is then required for steady-state fluid emission so that the pressure during deployment remains at 5 torr for a subsequent increase to 75 torr at full pressurization.

The Concept of the Inflation Capsule

The concept of the all-soft, double-chamber inflation capsule is based on the fact that the ejection of the inflation substance through a small orifice can be completed within a reasonably short duration only if the substance is ejected in liquid state. Gaseous ejection from a capsule that contains the boiling liquid would be unacceptably slow, unless a large orifice is provided, which, in turn, may result in explosive deployment if some liquid happens to be ejected.

The concept of the all-soft inflation capsule has been developed in response to the following operational requirements:

- In the packaged state, the capsule contains the inflation substance without any leakage into the brace volume.
- At ejection near the rocket's apogee, the capsule is actuated instantly to discharge all its liquid into the braces within a period of two to three seconds.
- The release and ejection operation is reliable.
- The operation of the capsule is independent of its orientation in the braces.

- The capsule is suitable for shelf storage of the packaged parachute (shelf life to be evaluated) and for exposure to a range of temperatures (to be determined).

- The capsule is all soft to minimize susceptibility of brace damage during rapid deployment.

- The capsule is lightweight and requires minimum packaging volume.

A schematic of the principal of operation of the inflation capsule is given in Figure 2. It consists of two concentric cylindrical volumes of similar diameter. The inner capsule contains the inflation liquid for ejection through a small orifice that is sealed by a peel-tab in the packaged state. The outer capsule contains a small amount of inflation liquid that will be used to accelerate the ejection by its pressurization. Schematically, the operation of the capsule involves three consecutive steps.

1. The packaged capsule (Fig. 2(a)) is released under vacuum conditions and at equal internal temperatures and capsule pressures ($T_0 = T_i$; $p_0 = p_i$).

2. The inner capsule inflates rapidly because its larger amount of liquid represents a larger reservoir of energy for evaporation ($T_0 < T_i$; $p_0 < p_i$). The peel tab is thereby removed from the ejection orifice.

3. The constant evaporation and gaseous ejection of inflation substance cools the inner capsule to a lower temperature than the outer capsule ($T_0 > T_i$; $p_0 > p_i$) which inflates against the inner capsule. Ejection of inflation substance in a liquid state is thereby greatly accelerated.

The entire process is nonstationary and is presumed to work only if it occurs at an appreciably faster rate than heat can be exchanged between the two capsules and their contents. Ejection times from 1.1 to 12 seconds have been measured, depending on orifice size, with 90% to 100% of the liquid discharged. An ejection time of two to three seconds is considered ideal.

Design of Experimental Capsules

Design and development of the most promising capsule has been guided by the following assumptions and considerations:

. Each brace leg carries one capsule at its tip. A parachute, therefore, has a total of four capsules.

. The selected pressurization substance is n-pentane. An amount of 5.3 cc (3.3 grams) of liquid is required for each capsule. The selection of n-pentane is based on an extensive review of a number of candidate liquids, including water, iso-pentane, diethyl ether, Freon-113 (and other types of Freon), methyl alcohol, etc. Water is safe and easy to use; its vapor pressure is, however, insufficient for full pressurization of the load-carrying braces. Iso-pentane develops high vapor pressures. Its sea-level boiling point is, however, lower than normal body temperatures; and, therefore, the liquid is difficult to handle.

Diethyl ether has attractive vapor pressures but is extremely flammable and an anesthetic. Freons are available over a wide range of attractive vapor pressures, and they are nonflammable; because of their high gas constants, however, all Freons require a substantial mass of liquid for pressurization. To develop the equivalent pressure of 3.3 grams of n-pentane, about 20 grams of Freon 113 are required; inflation capsules for Freon would, therefore, be quite heavy. Methyl alcohol is easy to handle but develops marginal vapor pressure for brace inflation.

. The basic capsule material selected is 2-mil, single-ply Mylar film. This thickness is recommended because of the considerable vapor pressures developed by n-pentane at elevated temperatures within the range typical for sounding-rocket payloads. The level of hoop stress in a pocket tube of 25-mm diameter under n-pentane vapor pressure of 70° C is of the order of 7.4×10^7 N/m^2 or 10,730 psi.

. After a limited number of early capsules of heat-sealable Mylar (Mylar-polyethylene laminate), heat sealing has been abandoned because of difficulties of control of bond quality, and du Pont 46970 polyester adhesive has been selected.

The evolution of the proper design of the inflation capsules necessitated the fabrication and testing of over 70 experimental units. A brief description of the experimental apparatus and a summary of experiments is given in Appendix B.

The most promising capsule design is summarized below. Bell-jar tests with this design have indicated a reliability of operation of 80 to 90 percent, and further environmental testing and parachute deployment testing are now indicated.

The capsule is made of clear 2-mil Mylar film. Du Pont 46970 adhesive (100 parts) is used with curing agent RC-805 (3 parts) and industrial grade methylene chloride (103 parts) to reduce viscosity. Furthermore, end seams are sealed with Schjelbond-100 polyester resin (0.5 mil thickness).

The capsule design is based on a folding pattern shown schematically in Figure 3. The axial seam is a simple lap joint (du Pont 46970). End seams are first sealed off by simple closure (du Pont 46970 - Schjelbond 100) followed by bending over and bonding (du Pont 46970). Dimensional layouts of the three major capsule elements are given in Figures 4, 5, and 6. Major steps of fabrication are shown in Figure 7. Injection of pentane into the capsules is accomplished at the following stages:

Outer capsule:	Fill in 0.35 cc prior to sealing of second seam of outer pocket.
Inner capsule:	Fill in 5.3 cc through filler hole after completion of capsule. Seal filler hole with circular patch (du Pont 46970). Vent all air out prior to closing.

It is recommended that the loaded inflation capsules be stored in the refrigerator, preferably under light compressive loading.

PARACHUTE PACKAGING AND DEPLOYMENT

The basic requirements of the packaging and deployment of Stokes-flow parachutes have been described extensively in References 2, 3, 4, and 5. Several schemes have been studied for the present application of inflatable X-brace parachutes to the Arcas or RDT & E sounding rocket, and the spiral packaging scheme has been developed and evaluated as the most promising approach. A number of features make this scheme particularly attractive. It embodies identical packaging procedures for either winddrifters or payload-carrying parachutes. It takes advantage of the fact that the flattened braces are comparable in size to the height of the cylindrical parachute container - a feature that makes any packaging with transversal brace folding ("spider" scheme) more difficult to implement. The spiral scheme minimizes creasing of the braces. It is suitable for closely controlled packaging on a large table surface and consists of a sequence of simple steps. It is ideally suitable for deployment under spinning conditions combined with controlled inflation starting from the brace tips. Because of its feature of individually folded canopy sails and separate location between the flattened braces, the susceptibility of canopy tangling is minimal, even under severe spinning conditions.

Sounding Rocket Integration

The packaged parachute is located between split staves in the clam-shell ejection canister developed by NASA-LRC for Arcas and RDT & E sounding rockets, see Figure 8. This canister provides for payload location in the rocket's nose cone and a split parachute container located in the cylindrical section immediately behind the payload/nose-cone assembly. The mode of ejection is payload first, axially forward. The parachute is released forward from the opened clam-shell canister. The parachute staves and top and bottom plates are made of lightweight Styrafoam cut or molded to the dimensions shown in Figure 8.

With these dimensions, some pressure packaging of the full-scale parachute of 14 m^2 area is required, and the packaging density achieved is close to 0.32 g/cc (or 20 lb/ft^3). It may be noted in passing that this packaging concept can be applied to parachutes up to approximately double the size of the present parachute if correspondingly thinner staves are used.

Direction of Rotation of Rocket

The direction of rolling of the braces during packaging in the spiral scheme requires coordination with the mode of axial rotation of the rocket to assure rapid deployment (see Fig. 9). It is assumed that the rocket spins in a clockwise direction. The braces are then rolled center-to-tip and counterclockwise, i.e., to the right, with the payload-suspension line assembly located on the right-hand side of the unrolled braces.

Preparation of Parachute Prior to Packaging

For payload-carrying parachutes, the single strap-on suspension line is looped over and across the brace manifold in the center of the parachute. With the brace located below the canopy, separation of the canopy center area of approximately 25 cm^2 is required so that the suspension straps can be threaded through.

Insertion of Inflation Capsules

Four loaded and properly sealed and leak-tested inflation cpasules are required. To minimize susceptibility of inadvertent capsule actuation during pressure packaging, the capsules are folded over once across the seal tab and the closed orifice. Then the folded capsules are inserted into the brace tips through an incision and secured by an external soft pin that will be removed after brace rolling. To facilitate pressure packaging, it is recommended that the capsules be located in alternating tip and bottom positions within the height of the flattened braces. After the insertion of the capsules, the incision is closed and sealed by a strip of Mylar.

The Concept of the Spiral-Packaging Scheme

In the spiral-packaging scheme each canopy sail (1/4 canopy located between adjacent braces) is rolled and flattened to a height approximately equal to the height of the flattened braces. The rolled sail is then placed between the adjacent braces which are stacked on top of each other. The entire package is then rolled center to tip (counterclockwise) and prepared for compression in the vacuum bag. The compressed and slowly evacuated parachute is then placed between the foam staves and inserted into the

clam-shell canister. A complete and detailed description of this procedure is given in Appendix C.

The entire packaging procedure has been implemented successfully a number of times with an experimental full-scale parachute with and without inflation capsules at its brace tips. During these experiments the following areas have been recognized as critical to successful packaging:

1. Careful folding of the canopy sails is required, and their even distribution between the flattened braces is a prerequisite for symmetrical packaging and positioning between the staves.

2. The vacuum bay should be evacuated slowly with ample time to form the compressed parachute by gentle massaging to a cylindrical shape. The last packaging procedures are performed with a commercial tire valve bonded to the vacuum bay along a large rubber flange.

3. Folding over of the inflation capsules prior to insertion, as described above, has virtually eliminated premature actuation during evacuation and packaging between the staves.

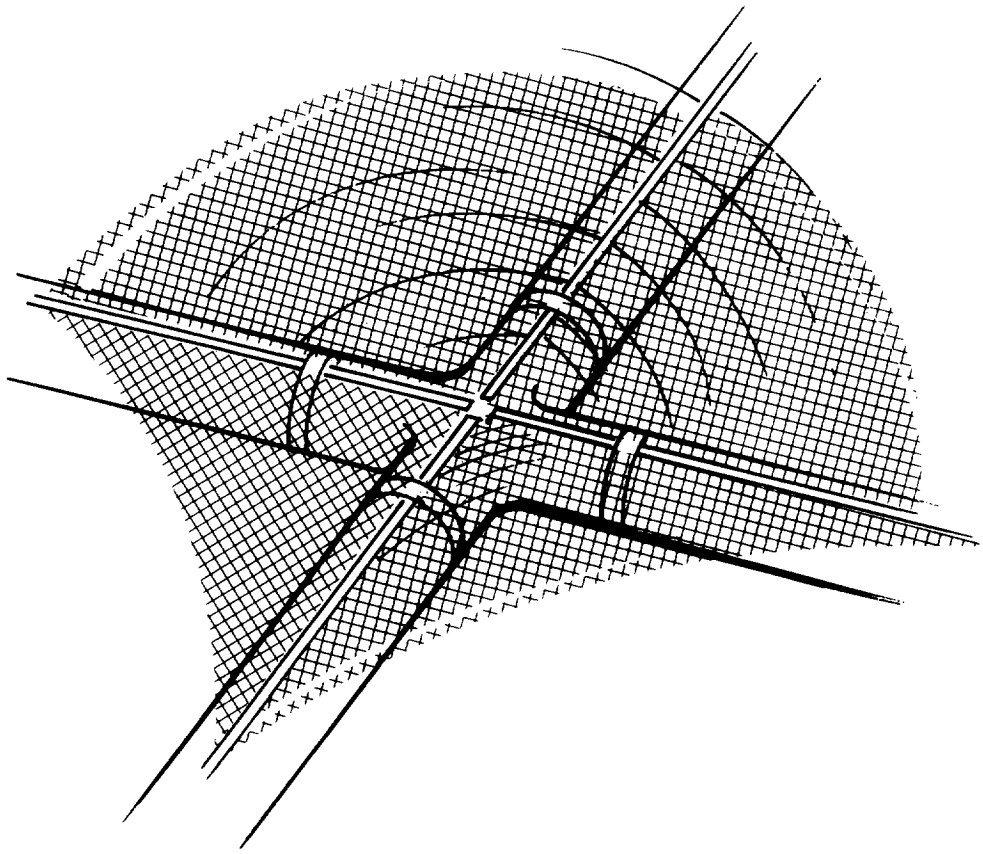

Figure 1. Center Manifold of Inflated Brace Structure

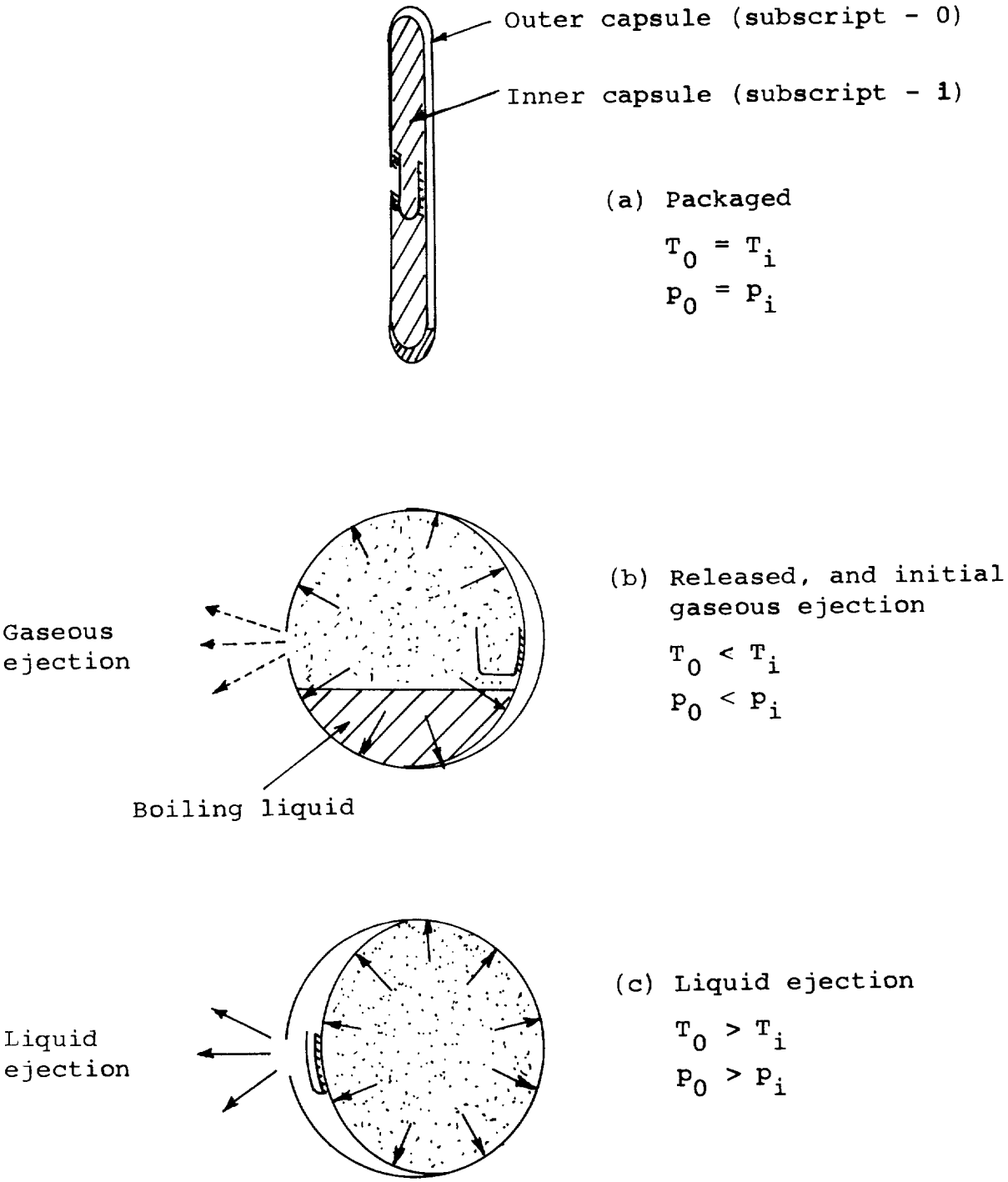

Figure 2. Schematic of Operation of Inflation Capsule

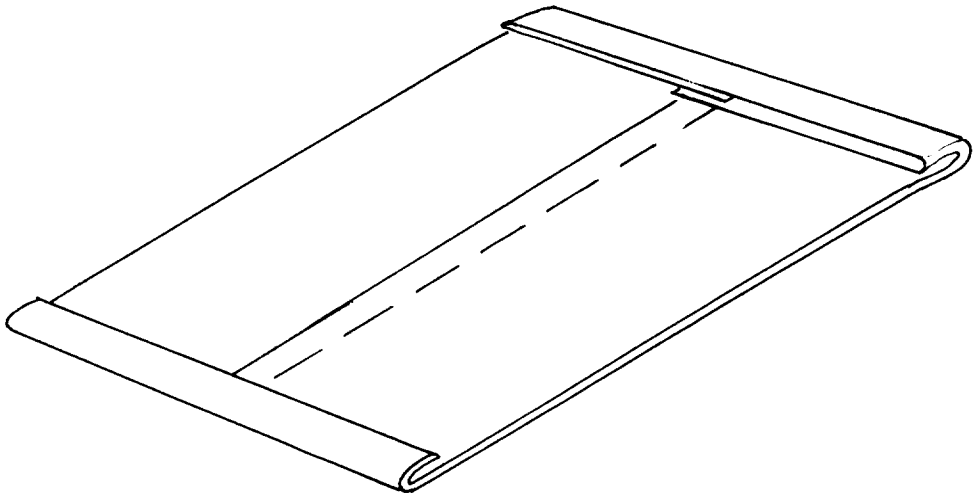

Figure 3. Basic Capsule Design

Note: All measurements in inches

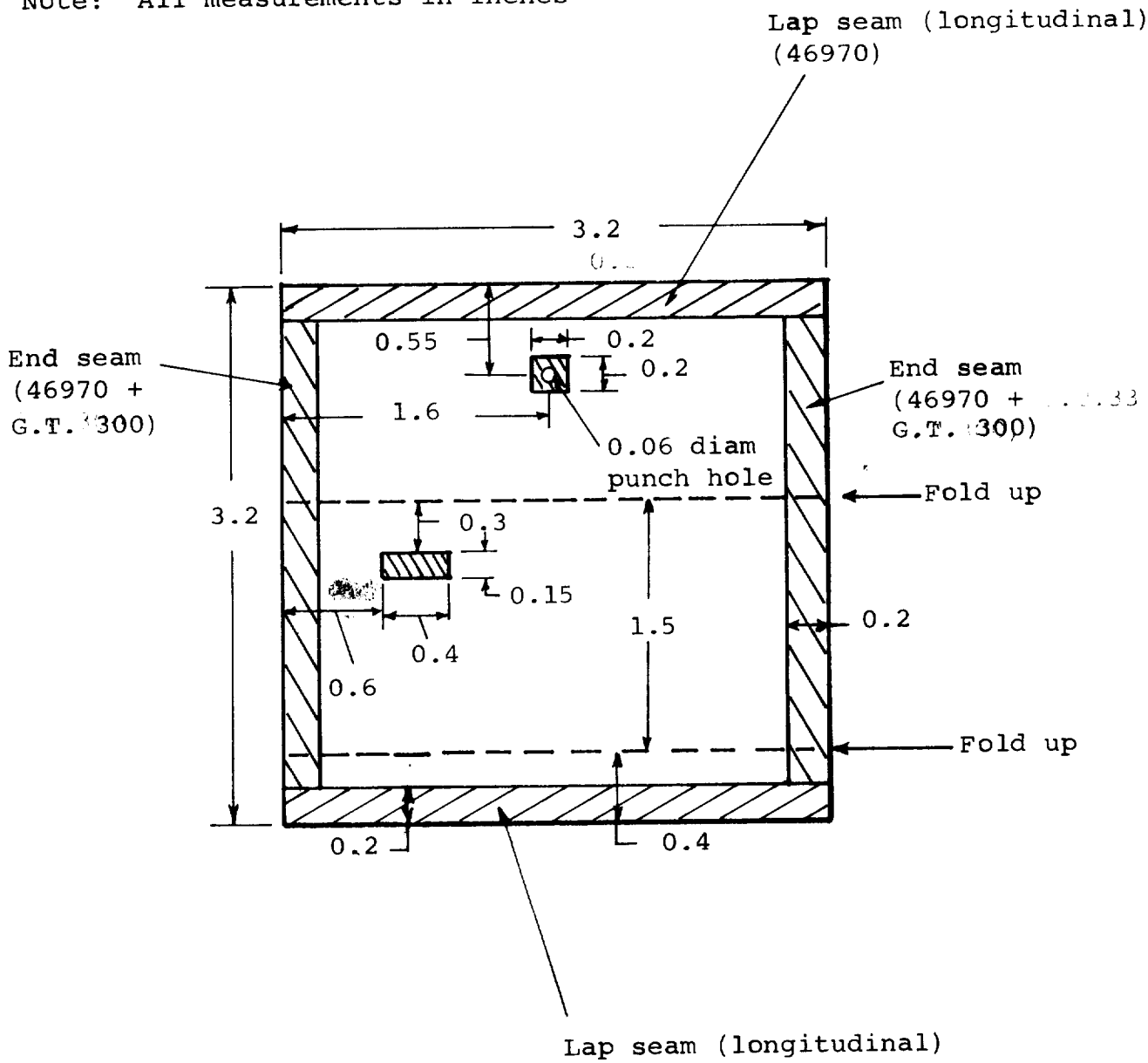

n-pentane: 5.3 cc (blue)

Figure 4. Layout of Inner Capsule

Note: All measurements in inches

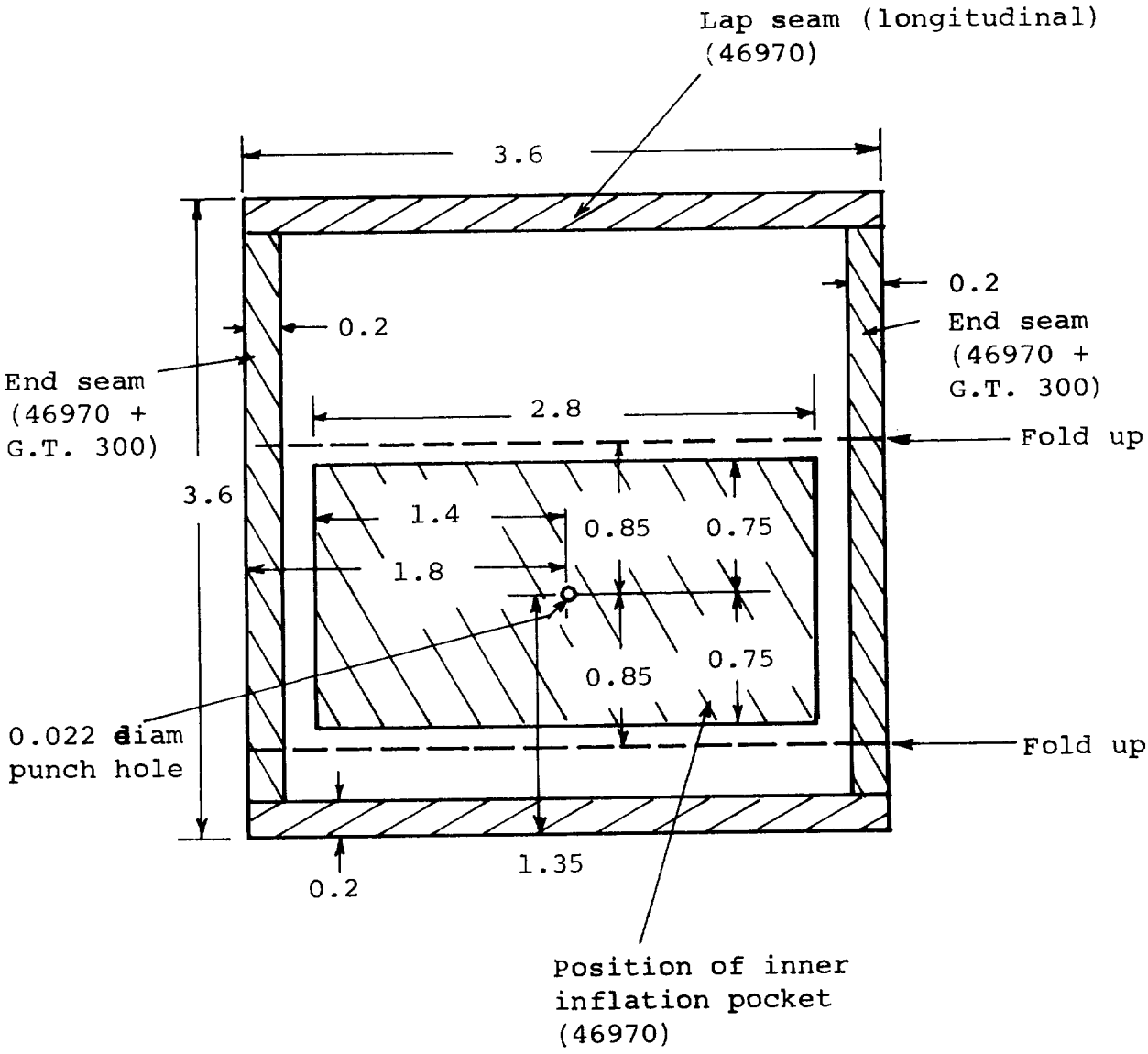

n-pentane: 0.35 cc (red)

Figure 5. Layout of Outer Capsule

Note: All measurements in inches

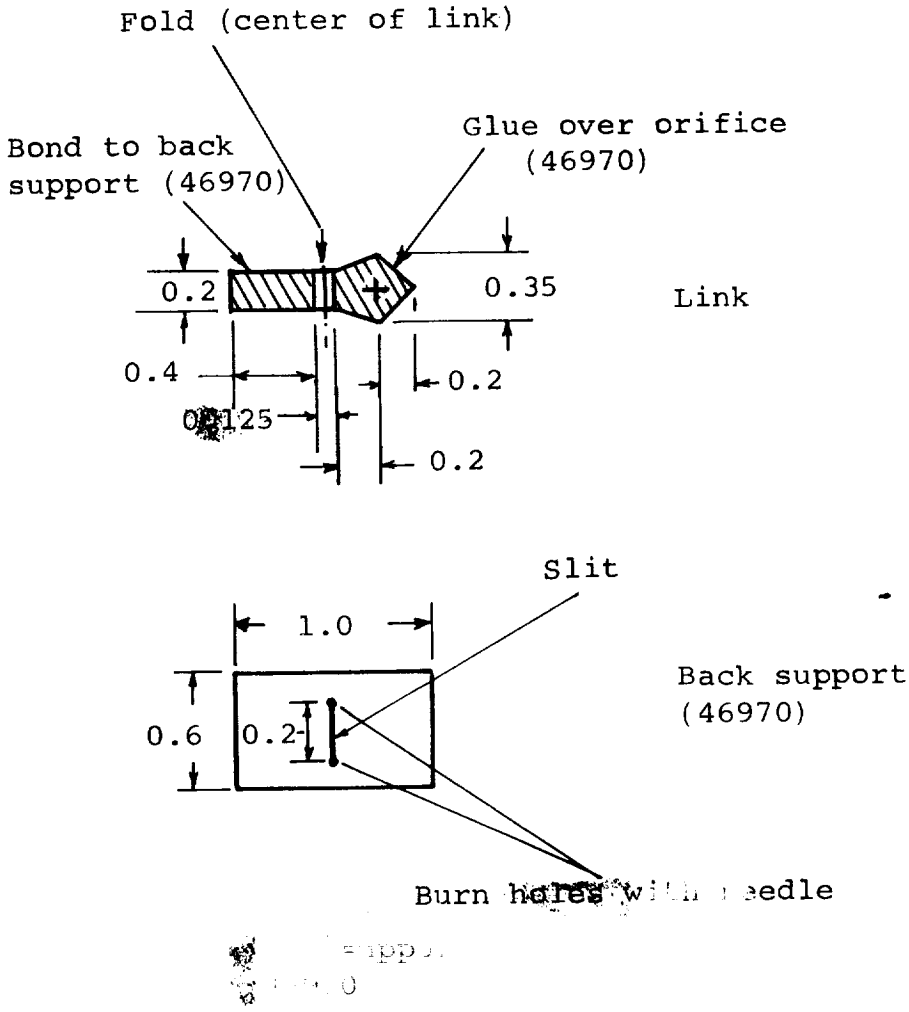

Figure 6. Layout of Roll Tab

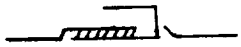

(a) Bond pull tab to back support

(b) Bond pull tab to inner capsule layout

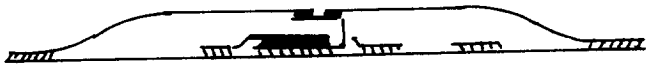

(c) Close inner capsule

(d) Bend end seams over

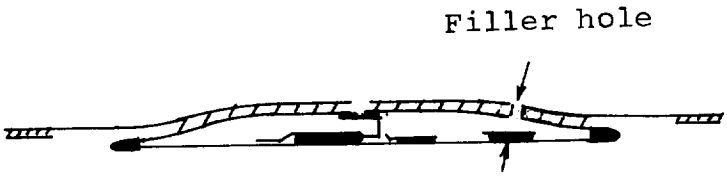

(e) Bond inner capsule to layout of outer capsule

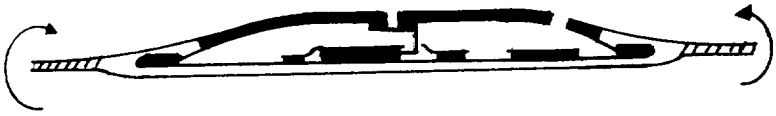

(f) Close outer capsule and bend end seams over

Figure 7. Steps of Capsule Fabrication

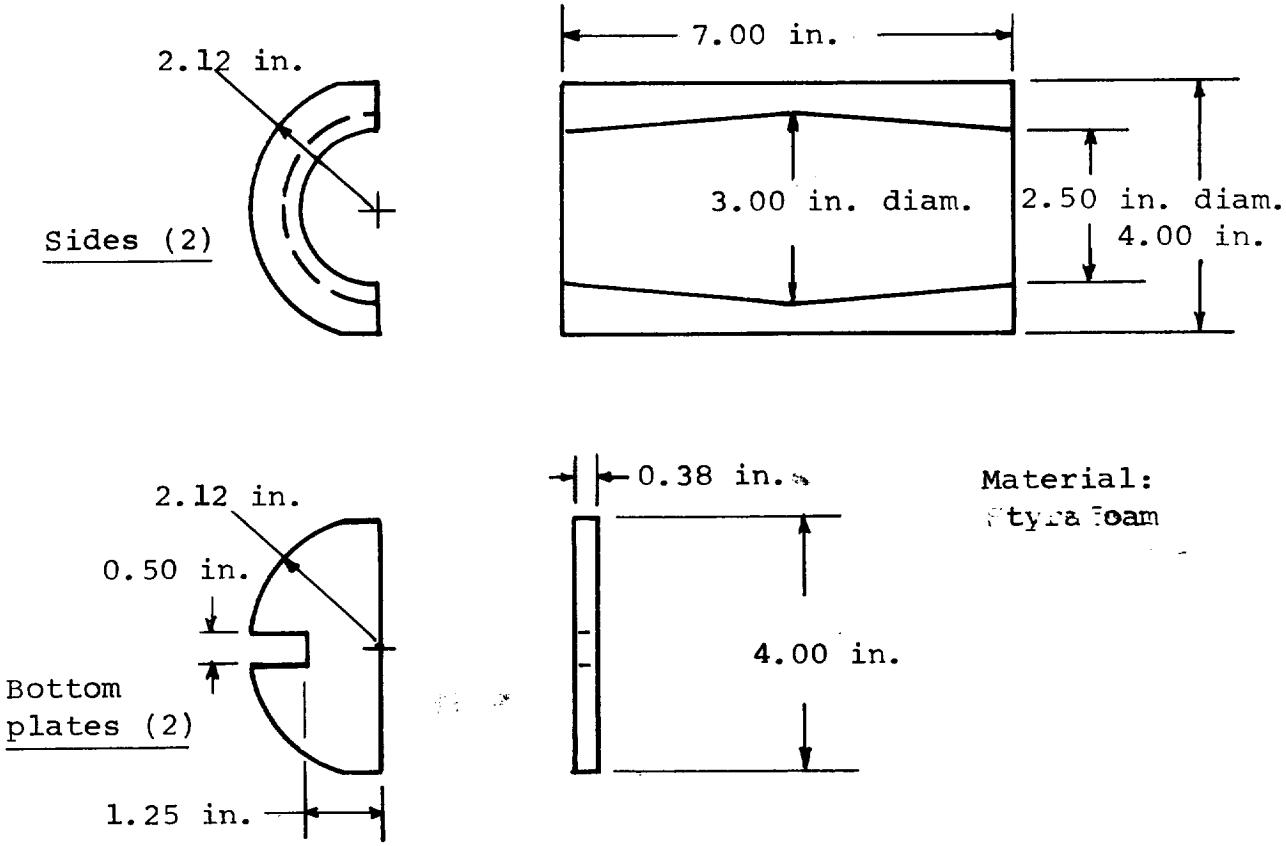

(a) Stave dimensions

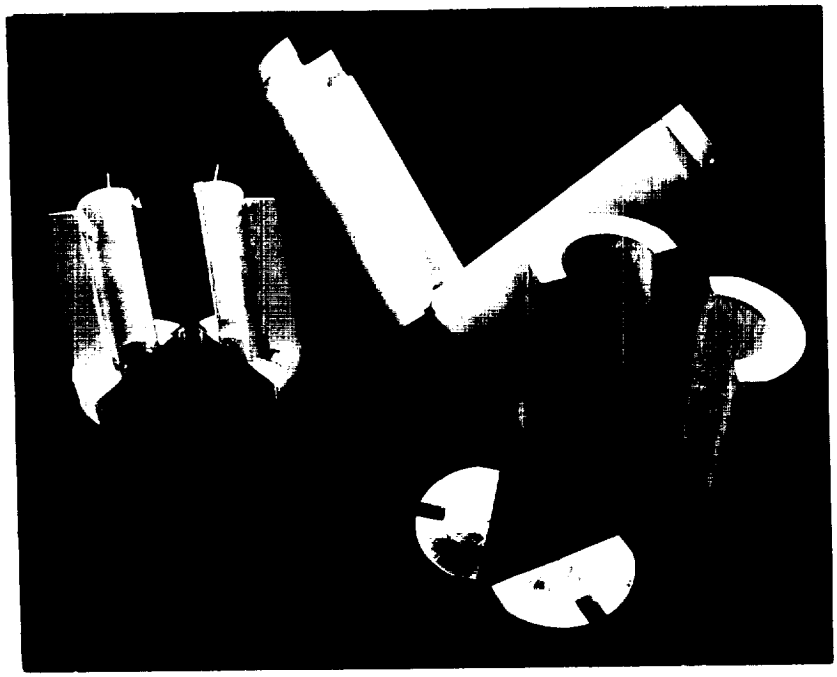

(b) Clam-shell with staves

Figure 8. Parachute Packing and Deployment Apparatus

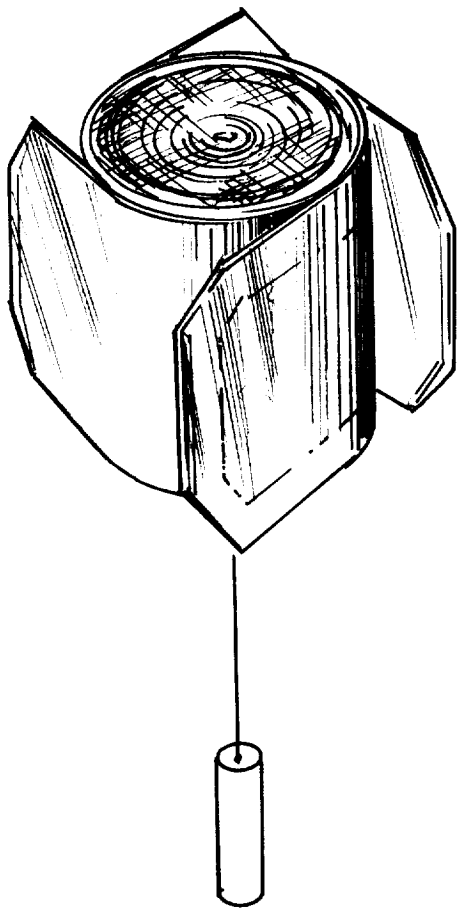

Figure 9. Packaging of X-Brace Parachute in a Spiral Wrap

APPENDIX A

DESIGN AND FABRICATION OF SINGLE SUSPENSION HARNESS

DESCRIPTION

The X-brace Stokes-flow parachute type X-14-4401 has a square canopy of 14 m^2 projected area, equipped with inflatable braces of 44 mm radius, and is designed to carry a small payload of 0.175 kg by a single central suspension line. The line consists of a simple harness assembly of Dacron ribbon that is strapped on the parachute prior to packaging. The harness design has been load tested statically up to 50 lb without permanent deformation or breakage. All parts used are standard, commercially available items.

Figure A-1 is a schematic of the general assembly, including suspension line dimensions. Design of brace harnesses is shown in Figure A-2. Figure A-3 illustrates loop sewing procedures, and Figure A-4 is a schematic of the attachment of harness to parachute.

LIST OF MATERIALS

(One Unit Suspension Assembly)

1. 145-lb test braided Dacron ribbon, 1/4 in. wide
   Supplier: Western Filament Corp.
   Brace harness: Two 32 in.
   Suspension line: One 9 ft-7 in.
   Total: 15 ft

2. 1 in. diameter key ring, steel, round, thickness 0.1 in.
   Supplier: Local locksmith

3. Heat sealable Mylar tape, one 1 mil, 1 in. wide
   Type Schjelbond 300 (resin on one side only)
   Supplier: G. T. Schjeldahl Corp.
   Brace harness cover: Four 15 in.
   Total: 5 ft

4. Heat sealable Mylar tape, 1 mil, 1 in. wide
   Type Schjelbond 300 (resin on one side only)
   Supplier: G. T. Schjeldahl Corp.
   Open end ribbon covers: Three 1 in. x 1 in.

5. Nylon sewing thread, Type A
   Supplier: Western Filament Corp.

RECOMMENDED STEPS OF FABRICATION

The implements necessary for fabrication include a standard sewing machine and associated equipment, and a flat-head heat-sealing iron which produces a temperature of 250° to 350° F.

1. Cut and mark dimensions for one suspension line (Figure A-1).

2. Cut and mark dimensions of end loop and Mylar covers for two brace harnesses (Figure A-2).

3. Cut four Mylar harness covers from tape, and six Mylar end patches (cut 1 in. square, round off later).

4. Prepare end loops and payload attachment loop by align-sewing areas and by fixing with Scotch tape.

5. Sew loops according to procedure illustrated in Figure A-3, including Steps 1, 2, and 3 in sequence. Use hand pull to assure stretched sewing areas.

6. Remove Scotch tapes.

7. Prepare and heat-seal brace harness covers as shown in Figure A-2.

8. Round off corners with scissors (Figure A-2).

9. Measure location of areas of attachment of brace harness to suspension line (Figure A-2). Make sure that both harnesses have same free length of 25 in. total $\pm$ 0.002 in.

10. Prepare key-ring loop and attachments of brace harness; align sewing area and fix with tape. Check for equal length of harnesses.

11. Sew according to procedure shown in Figure A-3, including Steps 1, 2, and 3 in sequence. Use hand pull to assure stretched and aligned sewing areas.

12. Remove Scotch tape.

13. Cut all loose ribbon ends and heat-seal under wrap-around Mylar patches.

14. Check assembly in accordance with Figure A-1; insert key ring into key-ring loop.

15. Weigh and package for storage in individual polyethylene bags.

ATTACHMENT TO PARACHUTE

The brace harnesses are looped loosely around the brace pressure manifold, as shown in Figure A-4. The braces are thereby assumed to be located below the canopy. The canopy is attached to the braces continuously, except for a length of 1 in. from the canopy center point.

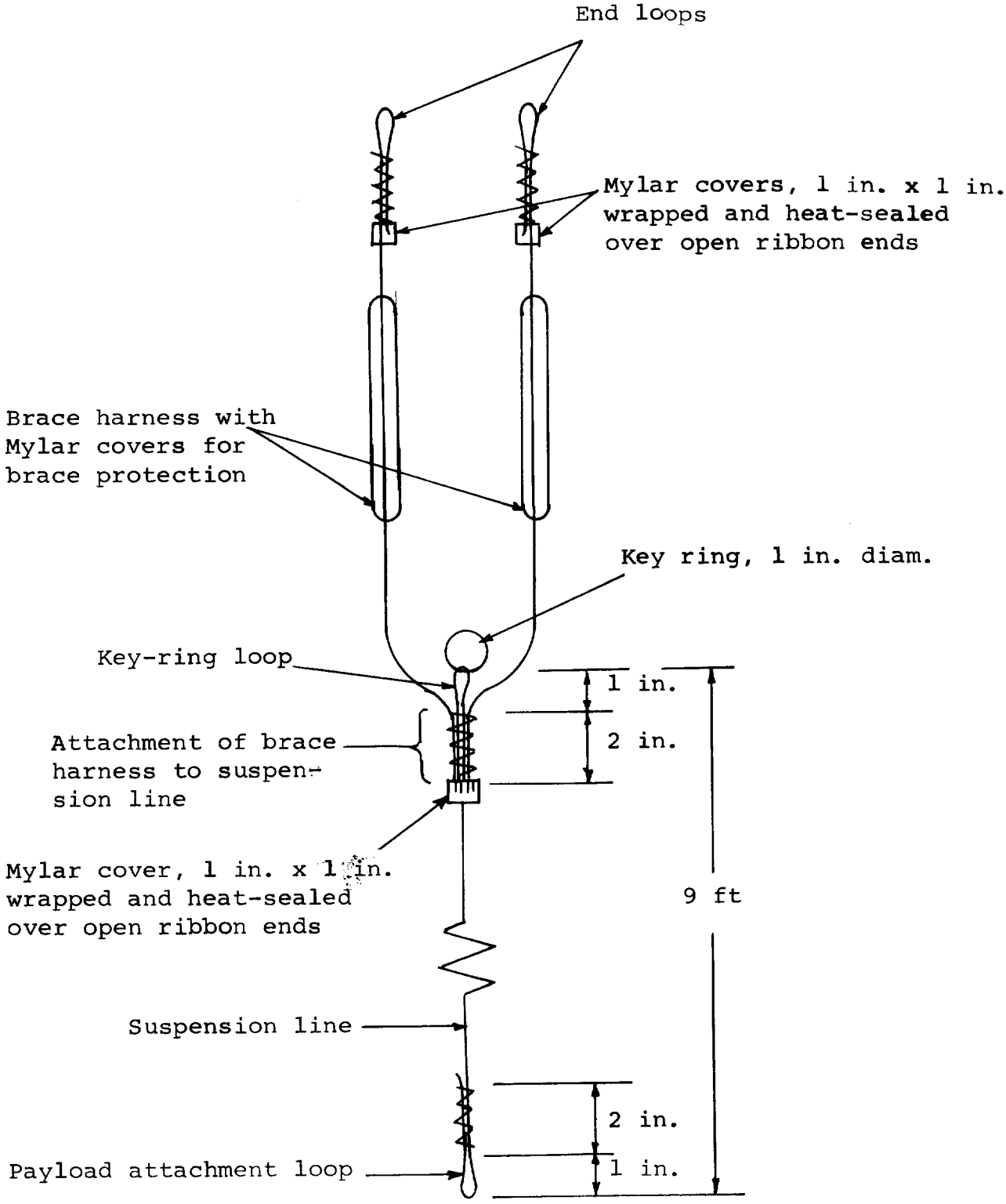

Figure A-1. Schematic of Suspension Line Design and Assembly of Suspension Harness

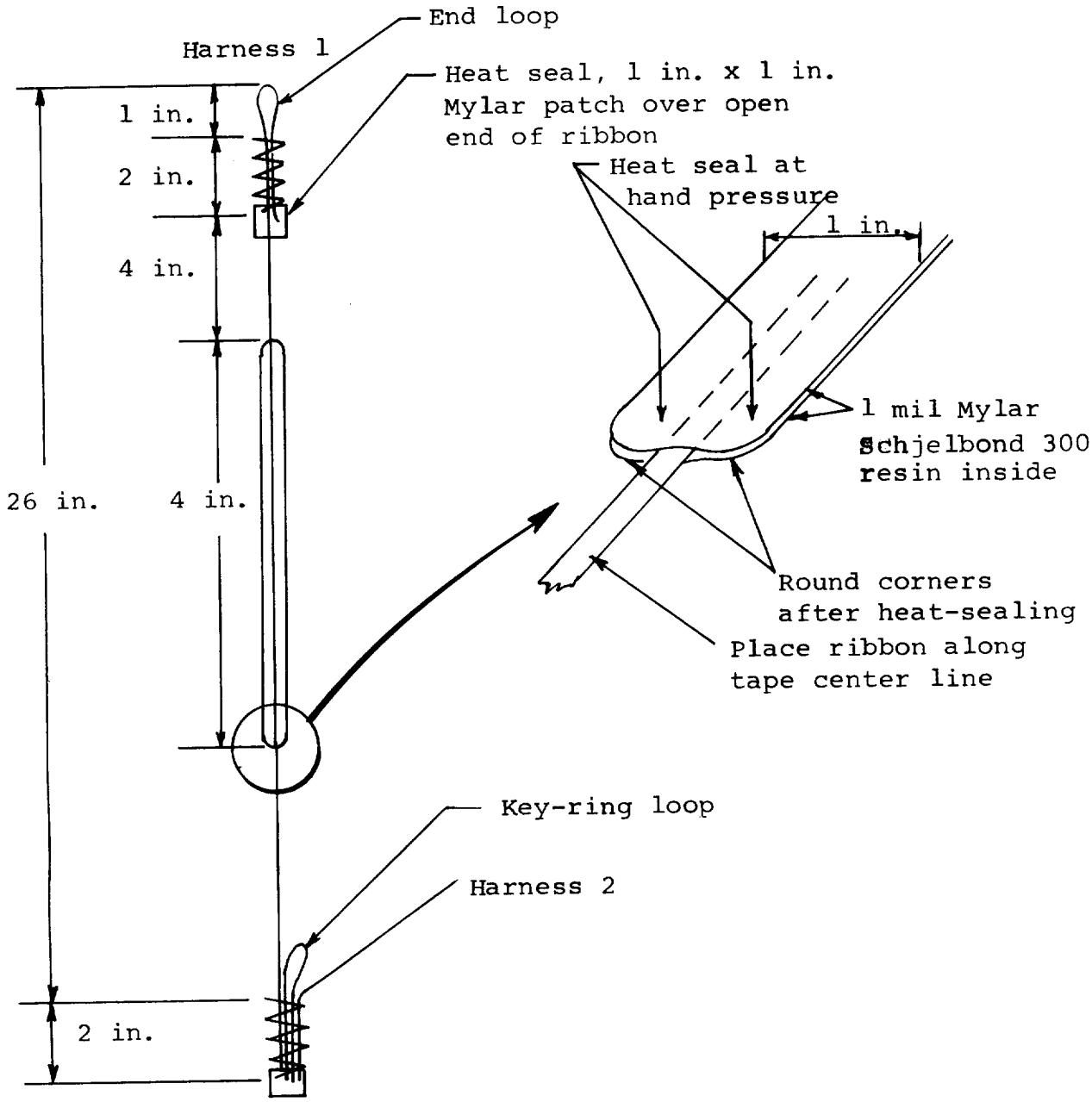

Figure A-2. Schematic of Brace Harness Design

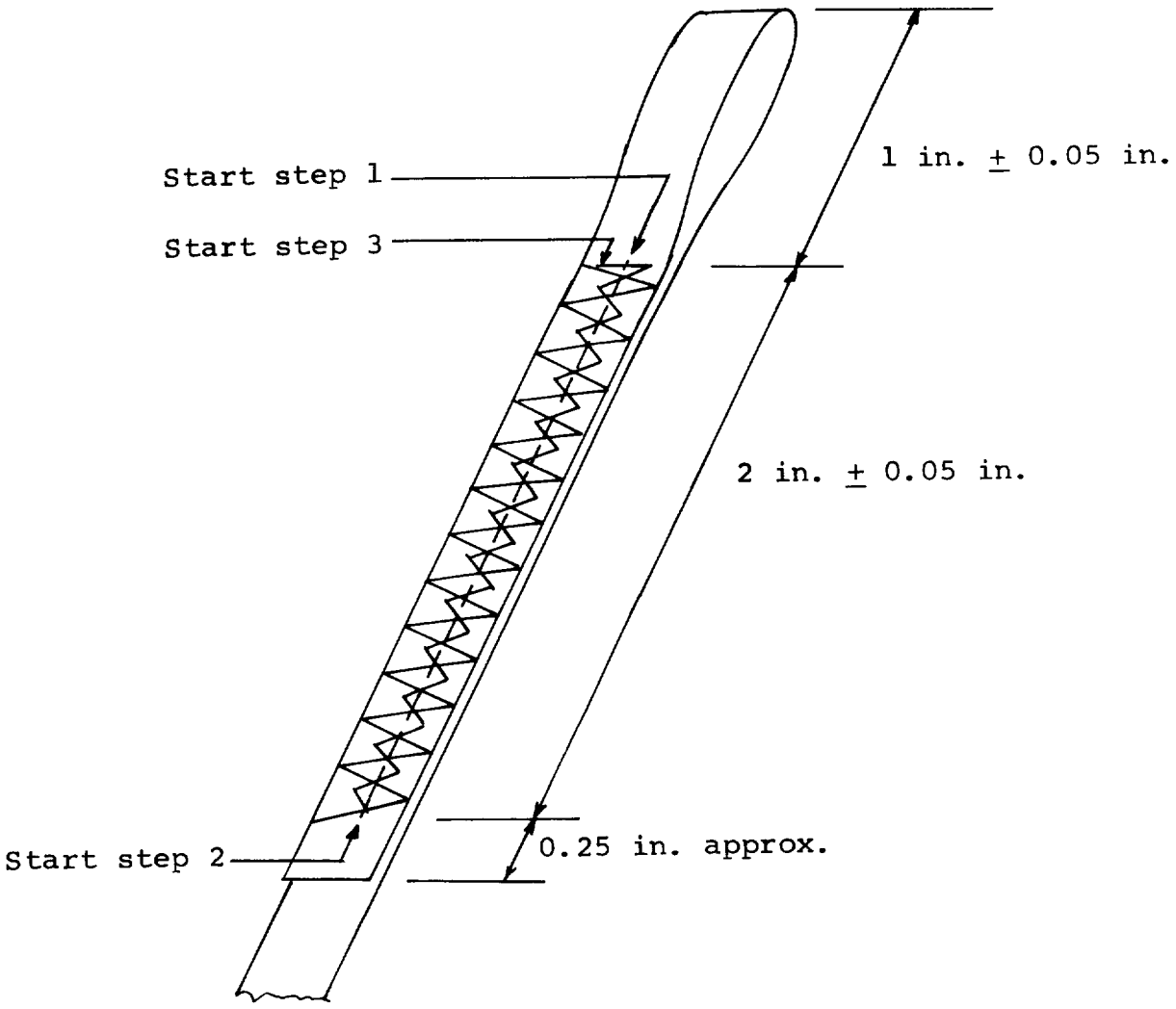

Definition of steps:

Step 1	Straight stitch	15 ±1 stitches/in.
Step 2	Zig-zag stitch	12 ±1 stitches/in. 0.1 in. wide
Step 3	Zig-zag stitch	10 ±1 stitches/in. 0.2 in. wide

Figure A-3. Standard Loop Sewing Procedure

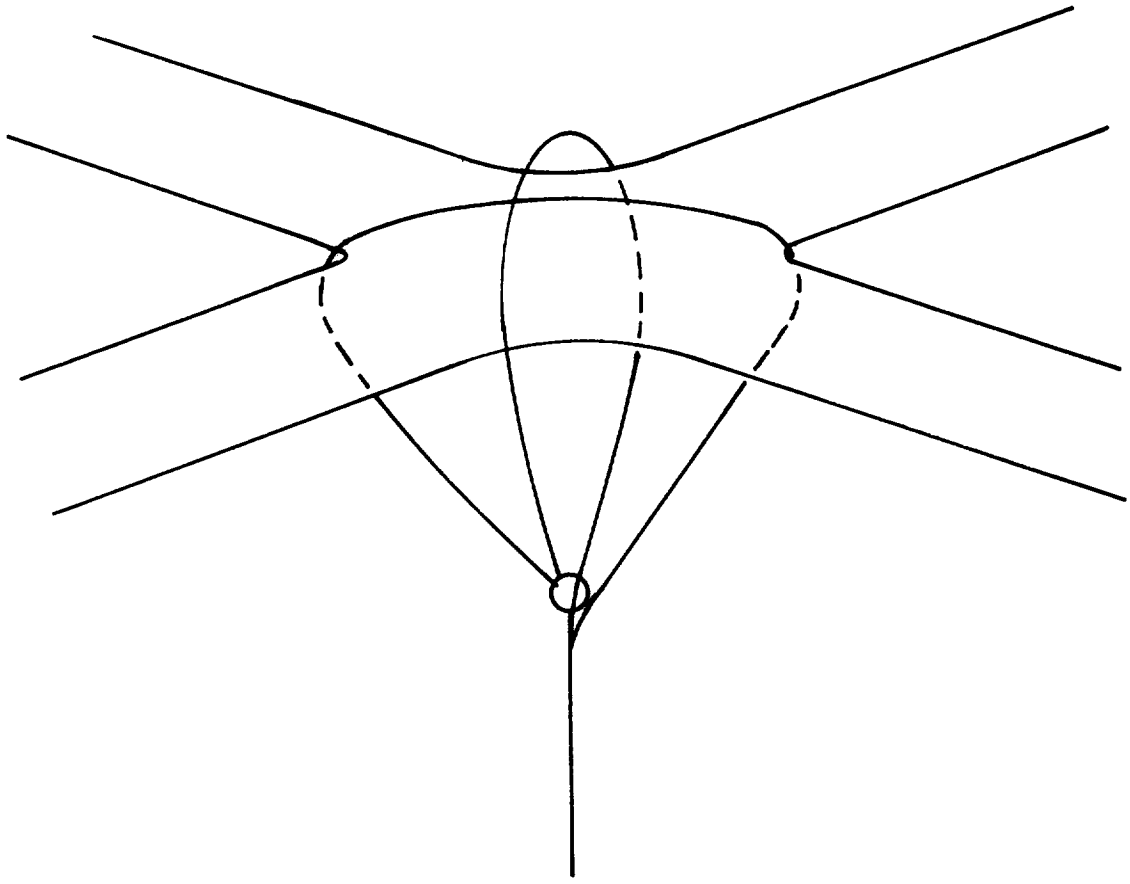

Figure A-4. Schematic of Attachment to Parachute

APPENDIX B

EXPERIMENTS WITH INFLATION CAPSULES

TEST APPARATUS

A test fixture was designed and fabricated to test the inflation pockets in a condition of simulated high-altitude deployment from a volume-restricted package. The device, shown in Figure B-1 consists mainly of two wooden blocks side by side, hinged along one end like a book. The blocks are approximately four-inches square, resting on a base block approximately five inches square. One block is pivoted at the bottom and held at the top by a latch. The gap between the blocks is 3.2 mm (1/8 in.). The test pocket is contained between the blocks and restrained from opening until the latch is released, which allows the blocks to separate.

Figure B-1(a) shows the test fixture in a vacuum-test bell jar with the latch in the closed position. The pocket at this point is exposed to vacuum but is restrained from opening. In Figure B-1(b) the latch has been opened so that the pocket expands and expels its fluid.

TEST RESULTS

Major problem areas encountered during the test period include:

- Compatibility of materials
- Seam leakage
- Premature orifice release
- No orifice release
- Seal-tab breakage
- Incomplete ejection.

Since preliminary answers to these problems have been found and successfully tested, the reliability of pocket operation has been increased greatly. However, further evolution and testing of capsules is clearly needed, primarily to facilitate pocket handling and to determine limits of environmental conditions under which the pockets will operate.

A complete list of tests is given in Table B-I and in Figures B-2 through B-9. Following are some detailed observations.

Total Emission

Total emission of the fluid has been obtained by:

1. Complete encapsulation of the emission chamber by the expulsion chamber
2. Anchoring of the emission chamber to the inside of the expulsion chamber to reduce wrinkling
3. Using proper amount of fluid in the expulsion chamber
4. Minimizing emission time so that heat transfer between the two chambers is low.

Leakage

During the testing period, an investigation was undertaken to determine the causes of and the remedies for pocket leakage. Test pocket No. 3 was selected for this test; from the outset it was losing mass at a rate of 1.3 mg/day (equivalent to 0.4 gram/year). As corrective action, it was dipped in a dilute solution of du Pont 46970 adhesive, but this resulted in a higher rate of loss. Further action taken was to coat this pocket with urethane epoxy, supplied by the Furane Comapny; leakage still persisted, and a possible pentane/urethane reaction was observed.

Pocket No. 3 was abandoned in favor of testing to determine permeability of pentane through Mylar. Several single pockets were fabricated with no escape hole. These revealed a permeability rate of less than 0.04 mg/day from a standard size pocket.

Leak tracing was accomplished by coloring the pentane with a felt marking pen (Carter's). Leak location becomes apparent due to the collection of ink dye at the site. With this method, it was found that major leaks occurred in the end seams. Remedial action was taken which eliminated this leakage. Schelbond 0.5-mil polyester resin film was inserted in the end seams in addition to the du Pont 46970 adhesive. All glued seams were cured under heat and pressure using a modified-tip soldering iron. Pockets now being fabricated by this method have undetectable leakage rate (< 0.1 mg in two weeks).

Rupture

Two types of rupture can occur: 1) tearing of the weak seal in the wrong location so that the emission hole remains closed, and 2) general tearing of the Mylar, causing either sudden full fluid emission or no emission, depending on which chamber is torn. The first problem has been solved by using strong material in the link (see Fig. B-9) and exposing the hole by peeling the link away (the peel orientation results in a weak seal of consistent strength). The use of 2-mil Mylar in the entire pocket, except for the link which is 5-mil Mylar, has solved the second problem.

Reliability

The pockets as presently designed (Fig. B-9) are reliable in that full emission has been achieved and that rupture and general

leaks have been eliminated. A problem still to be resolved is one which occurs during filling in which the weak seal comes apart prematurely, allowing the fluid to escape. It may be possible to remedy this by exercising more care during fabrication and filling.

TABLE B-I. TEST SERIES OF THE DOUBLE-WALL POCKETS

Pocket No.	Figure No.	Δt (sec)	Emission (%)	Comments
1	B-2			No emission; back of seal peeled away
2	B-2			No emission; back of seal peeled away
3	B-2			Saved for leak test
4	B-2			No emission; back of seal peeled away
5	B-2	2.5	90	
6	B-3	2.5		Ten second delay before seal opened
7	B-4			Didn't open
8	B-5			Didn't open
9	B-4			Leaked inside to outside
10	B-4			No record
11	B-4	5	90	
12	B-4			Square pocket - inside wrinkled
13	B-4			Square pocket - leaked inside to outside
14	B-6		70	
15	B-5			Inside wrinkled
16	B-5		82	
17	B-5			Didn't open
18	B-5	7	70	
19	B-5			Didn't open
20	B-5			Didn't open
21	B-7	2.1	100	
22	B-4			Outside leaked out
23	B-7	8	97	
24	B-7	3	100	

(continued)

TABLE B-I (sheet 2)

Pocket No.	Figure No.	Δt (sec)	Emission (%)	Comments
25	B-7			Didn't open
26	B-7			Didn't open
27	B-7			Didn't open
28	B-7			Leaked inside to outside
29	B-8			Outside leaked out
30	B-8	5	100	
31	B-8	2.5	80	
32	B-8			Outside leaked out (hole opened)
33	B-8	5.5	90	
34	B-8			Link broke
35	B-8	4.5	97	
36	B-8	6	98	
37	B-8			Leaked inside to outside
38	B-8			Link broke
39	B-8			Outside leaked (hole opened)
40	B-8	11	95	
41	B-8			Outside leaked out (hole opened)
42	B-8			Link broke
43	B-8			Link broke
44	B-8			Inside leaked out
45	B-8			Link broke
46	B-8			Outside leaked out (hole opened)
47	B-8	6.5	90	
48	B-8	3.2	93	
49	B-8			Outside leaked out (hole opened)
50	B-8			Outside leaked out (hole opened)

Note: Pocket No. 29 - 47: 2-mil Mylar link
Pocket No. 48 - 50: 5-mil Mylar link

(continued)

TABLE B-I (sheet 3)

Pocket No.	Figure No.	Δt (sec)	Emission (%)	Comments
51	B-8			Outside leaked out (hole opened)
52	B-8			Outside leaked out (hole opened)
53	B-8	>20	100	
54	B-8	4.5	100	
55	B-8	>20	90	
56	B-8	6.7	98	
57	B-8	10	100	
58	B-8			Leak test
59	B-8	6	100	
60	B-8			Leak test
61	B-8			Back of link tore away
62	B-8			Leak test
63	B-8	9	100	
64	B-8			Dirty hole; outside leaked out
65	B-8			Dirty hole
66	B-8			Back of link tore away
67	B-9	2.5	95	
68	B-9	2.5	95	
69	B-9	2.2	95	

Note: Pocket No. 51 - 69: 5-mil Mylar link

(a) Closed

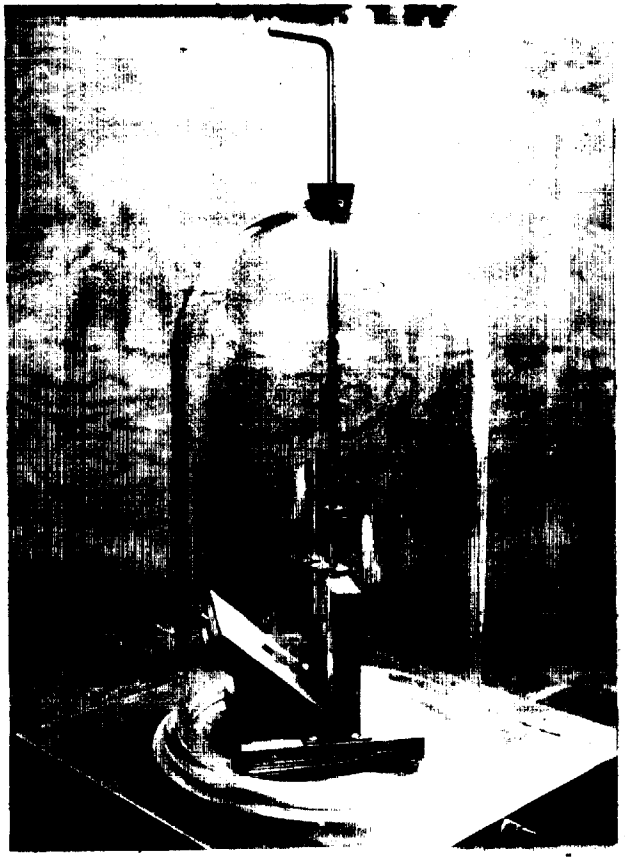

(b) Open

Figure B-1. Inflation Capsule Testing Apparatus

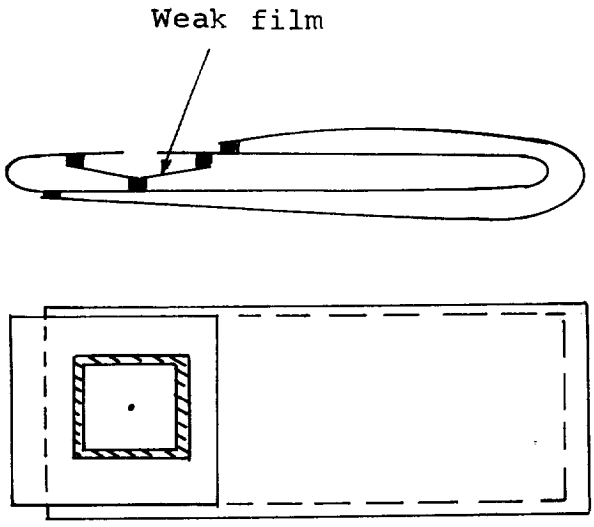

Figure B-2. Pocket Configuration: Tests 1 - 5

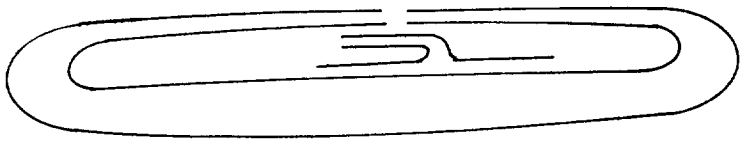

Figure B-3: Pocket Configuration: Test 6

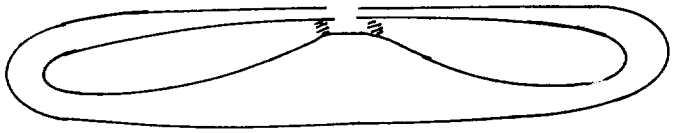

Figure B-4. Pocket Configuration: Tests 7, 9-13, 15-20, and 22

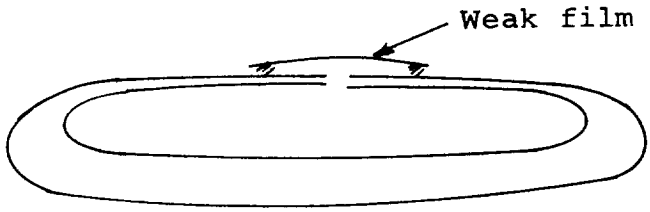

Figure B-5. Pocket Configuration: Test 8

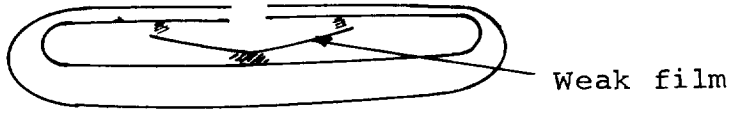

Figure B-6. Pocket Configuration: Test 14

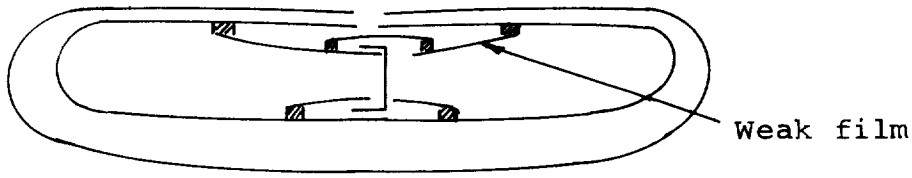

Figure B-7. Pocket Configuration: Tests 21, 23-28

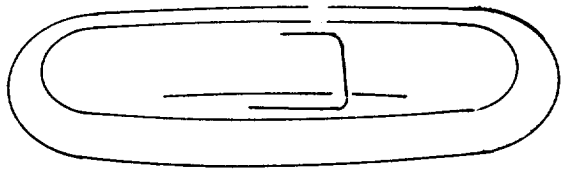

Figure B-8. Pocket Configuration: Tests 29-69

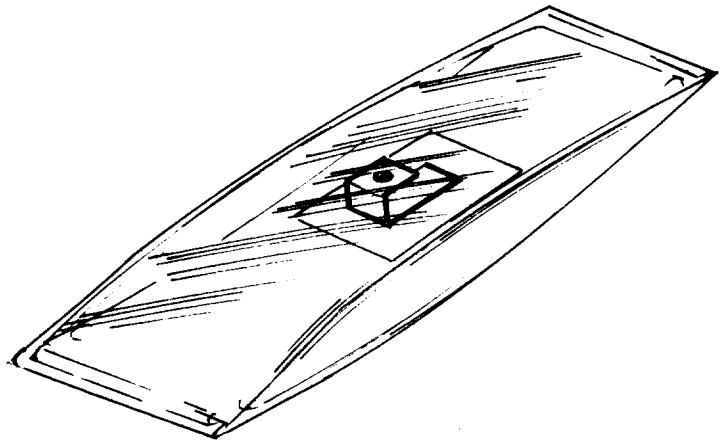

(a) Capsule in a nonruptured state

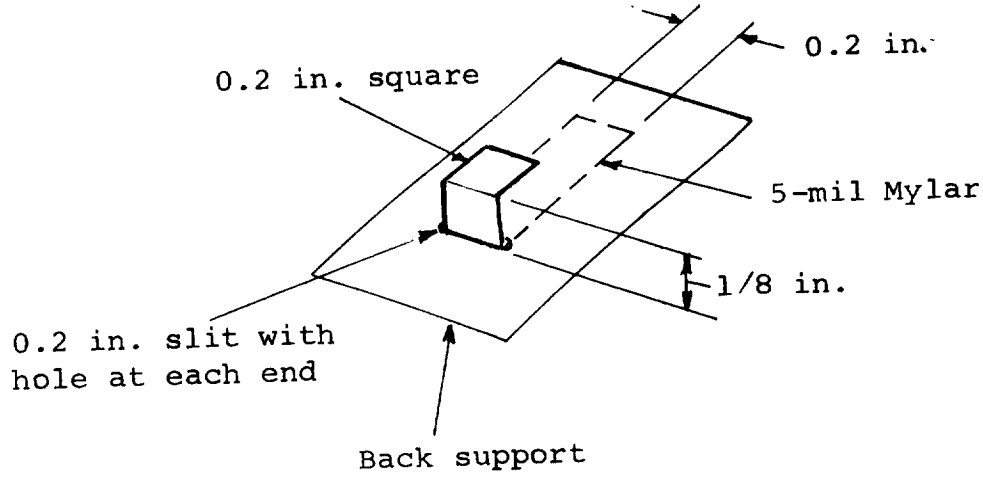

(b) Hole release link and back support

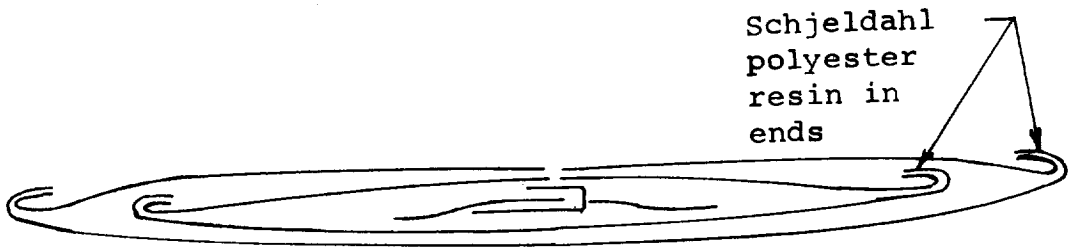

(c) Schematic side view

Figure B-9. Present Inflation Capsule Design

APPENDIX C

PACKAGING INSTRUCTIONS - 14 METER^2 PARACHUTE

CONCEPT

The full-scale (14 m^2 area) Stokes-flow parachute is packaged so that it deploys spirally. This Appendix gives complete instructions for packaging, with figures and material specifications, beginning with the parachute flat on a table and progressing to the final stage in which the parachute is inside the canister with its staves in place.

MATERIALS

Materials necessary for packaging are:

1. Parachute, complete with inflation pockets, and suspension line if needed
2. One yardstick or meter-stick
3. One folding guide (7 in. x 8 ft x 1/8 in. Plexiglas with rounded edges)
4. One "Ziploc" gallon-size polyethylene bag (Dow Chemical Co.)
5. A piece of sheet rubber 1-in. square x 1/16 in. thick
6. "Spra-ment" adhesive (3M Scotch Brand)
7. Tygon tubing 1/4 in. diam x 1 in. long
8. One syringe needle
9. Vacuum pump
10. Staves and split bottom plate, described in Figure 8
11. Clam-shell canister (See Fig. 8)
12. Aluminum canister (see Fig. C-2(e))

DETAILED SEQUENCE

Folding for Spiral Packaging

The following instructions explain packaging, up to hand rolling of the folded parachute:

1) Spread the parachute on large table so that the brace tubes are beneath the mesh; number them clockwise, as shown in Figure C-1(a).

2) Fold the parachute through its center so that brace legs 2 and 3 lie on brace legs 1 and 4 (see Fig. C-1(b)).

3) Prepare the gore which is between brace legs 1 and 2 for folding by placing brace legs 1 and 2 side by side with a 2-in. gap between them (see Fig. C-1(c)). Note that brace leg 2 is on top of the mesh.

4) Complete preparation by moving brace leg 2 back on top of brace leg 1, creating a space into which the folded mesh is to be placed (see Fig. C-1(d)).

5) Fold the gore so that it is in a roll of 7-in. width, using the folding guide and the yardstick, the latter to position the folds properly so that the last fold lies between brace legs 1 and 2 (see Fig. C-1(e)).

6) Place the gore between brace legs 1 and 2 (see Fig. C-1(f). The tucked-in gore should lie evenly, with the mesh protruding 0.5 to 1.0 in. from the sides of the brace tubes.

7) Prepare the next gore which is between brace legs 2 and 3 for folding. Place brace leg 3 next to the already folded mesh with a 9-in. gap between them (see Fig. C-1(g)). Note that brace leg 3 is under the mesh.

8) Move brace leg 3 back on top of brace leg 2, as in Step (4). Fold the gore in a 7-in. roll, using the folding guide and yardstick, as in Step (5) (see Fig. C-1(h)).

9) Place the gore between brace legs 2 and 3, taking care that the mesh lies evenly and protrudes from the sides of the brace tube legs, as in Step (6) (see Fig. C-1(i)).

10) Prepare the next gore which is between brace legs 3 and 4 for folding. Place brace leg 4 next to the already folded mesh with a 2-in. gap between them (see Fig. C-1(j)). Note that brace leg 4 is on top of the mesh. The varying mesh/brace tube orientation in Steps (3), (7), and (10) is the reason for the different instructions in these steps.

11) Move brace leg 4 back on top of brace leg 3, as in Step (4). Fold the gore in a 7-in. roll, using the folding guide and yardstick, as in Step (5) (see Fig. C-1(k)).

12) Place the gore between brace legs 3 and 4, taking care that the mesh lies evenly and protrudes from the sides of the brace tube legs, as in Step (6).

13) Accordian-fold the final gore which is between brace legs 4 and 1, on top of brace leg 4 (see Figs. C-1(ℓ) and C-2(a)).

14) Roll the parachute toward the brace leg ends, keeping the suspension line on the right as viewed in the forward direction of roll. Roll loosely, using care that minimal finger pressure is exerted on the inflation pockets.

Insertion of Spiral Package Into Canister

The following instructions explain compaction of the hand-rolled parachute and its placement in the deployment canister. Steps (15) through (17) are for preparation of an evacuation bag; Steps (18) and (19) cover parachute compaction.

15) Using the "Spra-ment" adhesive, attach the 1-in. square of sheet rubber on the outside of a "Ziploc" bag, near the open end.

16) Place the parachute in this bag so that the free suspension line is toward the open end of the bag (see Fig. (C-2(b)). Put all of the suspension line in the bag, and put the piece of tubing in the bag near the rubber patch to protect the bag and contents from puncture by the needle.

17) Insert the syringe needle through the rubber into the bag, with the protective tubing surrounding the needle.

18) Evacuate the bag through the syringe needle (see Fig. C-2(b)). During evacuation adjust the parachute shape so that it remains generally cylindrical (wrinkling occurs here).

19) The parachute in the compacted state is slightly barrel-shaped (7-in. long, 2.5-in. diameter at the ends, 3-in. diameter in the middle). When this state is reached, remove the syringe needle (Fig. C-2(c)).

20) Place staves around parachute. Allow sides of "Ziploc" bag to protrude through stave separations. Place parachute and staves (including split bottom stave plate) into clam-shell, again allowing the bag to protrude through the slits (Fig. C-2(d)).

21) Using strong tape to prevent the clam-shell from opening, cut the "Ziploc" bag flush along the sides and across the top of the clam-shell. Slide clam-shell into metal canister during this operation (Fig. C-2(e)).

22) Thread the suspension lines through the hole in the top portion of the clam-shell, and attach the payload (if any).

23) Join the top and bottom portions of the clam-shell (see Fig. C-2(f)).

FULL-SCALE VACUUM DEPLOYMENT TEST

On November 3, 1971, a full-scale deployment test was performed with a spiral-packed 14 m^2 Stokes-flow parachute carrying a dummy payload. The test was performed in the NASA-LRC 41-foot vacuum sphere. The parachute used water as inflation substance stored freely in the brace volume (no capsules). Test conditions were:

Chamber pressure:	Less than 1 torr
Velocity of ejection from canister:	Approximately 50 ft/min
Spin rate:	Approximately 1500 rpm

Deployment was vertically downward from the ceiling of the chamber. Deployment action was recorded by several cameras operating at 400 frames per second. A height of approximately 10 to 15 feet was available for the parachute to deploy before impacting.

Upon release from the clam-shell, the parachute deployed immediately to 75 - 90 percent of its full size before impacting.

Deployment of all braces was even, and the parachute nearly stopped spinning before impact. The parachute appeared well pressurized immediately after impacting, but collapsed immediately thereafter. The reason for the collapse was later identified in the movie - it was caused by a small particle of the payload shell. Inspection of the parachute immediately after pressurization of the chamber showed no tangling of the suspension line, no extensive brace damage where the particle impacted, no canopy tangling, and no major mesh damage.

The test demonstrated the successful operation of the spiral packaging and deployment scheme under simulated ejection conditions using uncontrolled pressurization with water vapor.

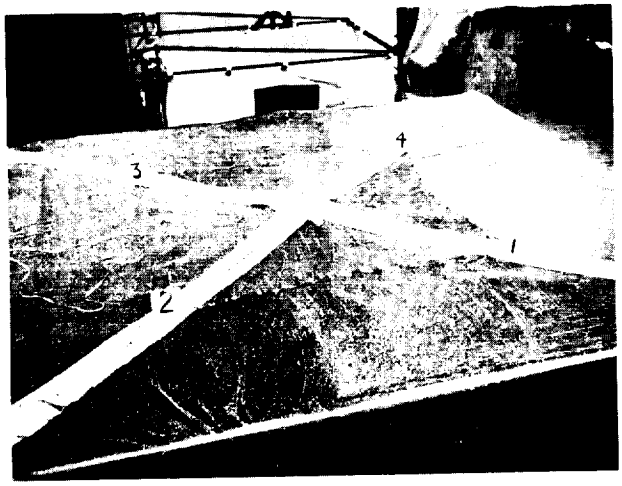

(a) Parachute on table

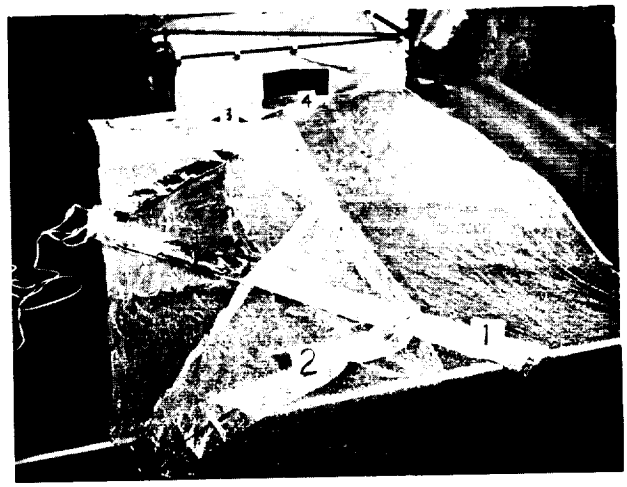

(b) Initial fold

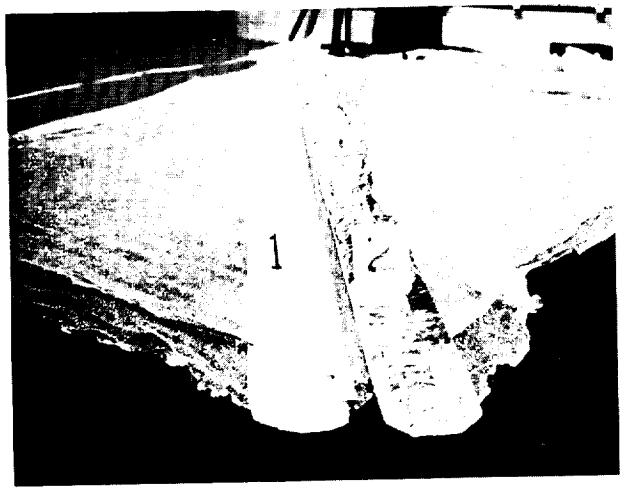

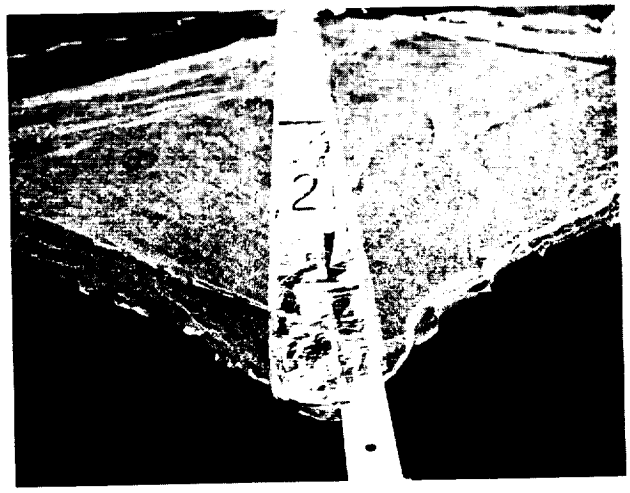

(c) & (d) Preparation for folding of first gore

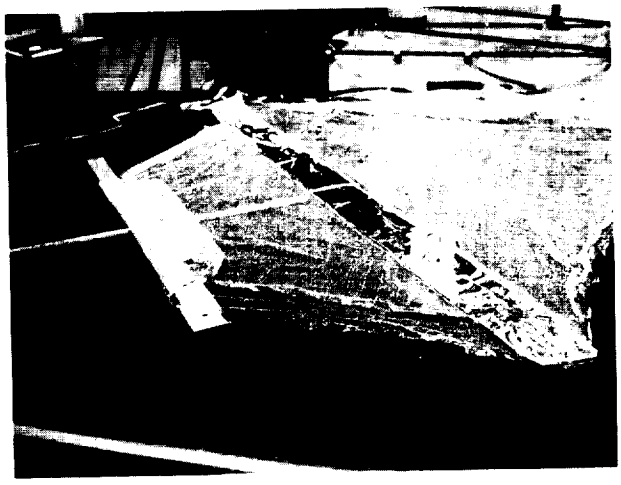

(e) Folding first gore

(f) Placement of first gore

Figure C-1. Folding for Spiral Packaging of 14 m^2 Parachute

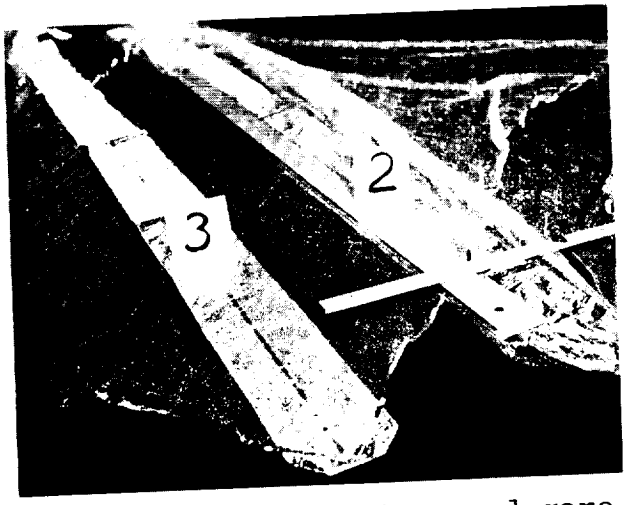

(g) Preparation of second gore

(h) Folding second gore

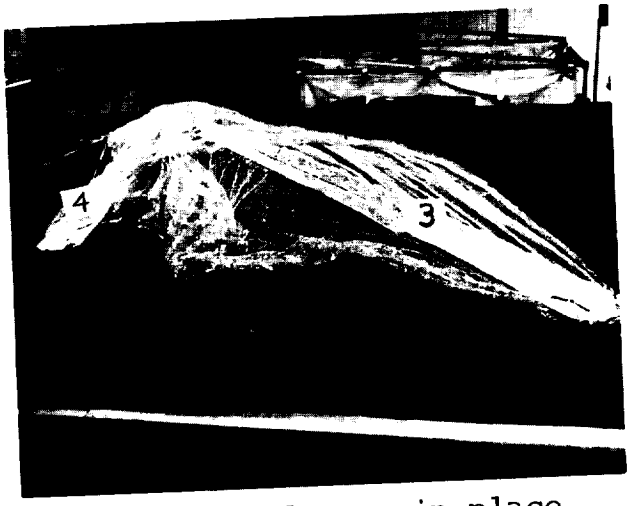

(i) Second gore in place

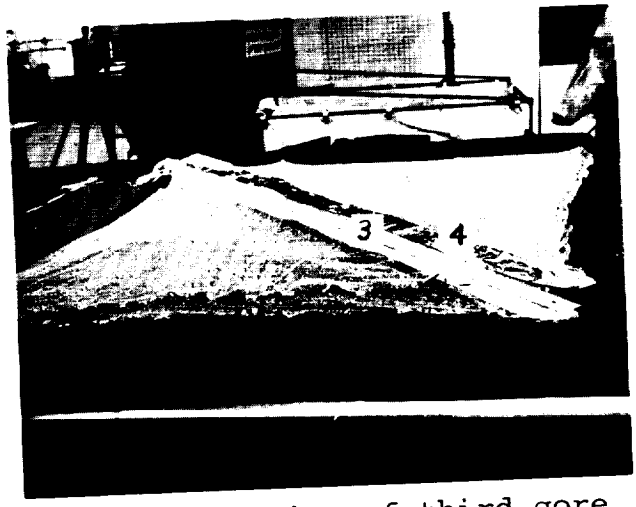

(j) Preparation of third gore

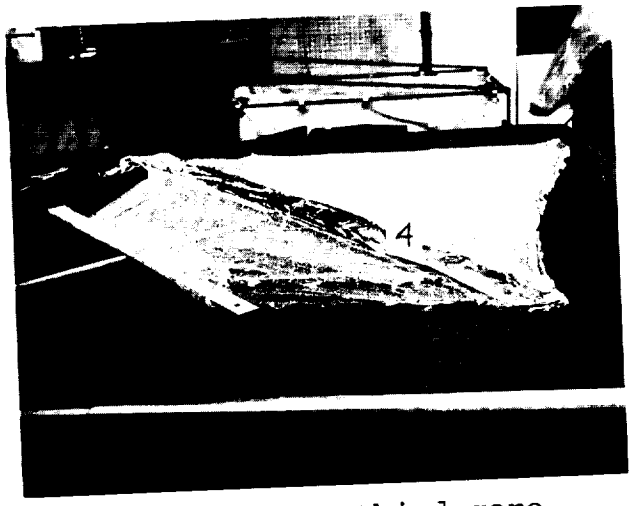

(k) Folding third gore

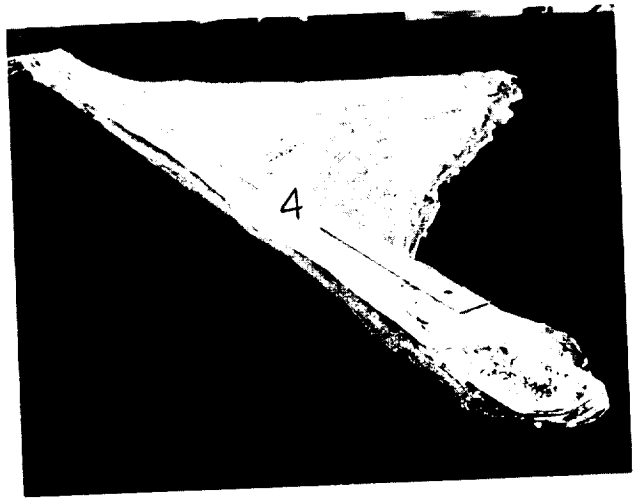

(ℓ) Folding fourth gore

Figure C-1. (continued)

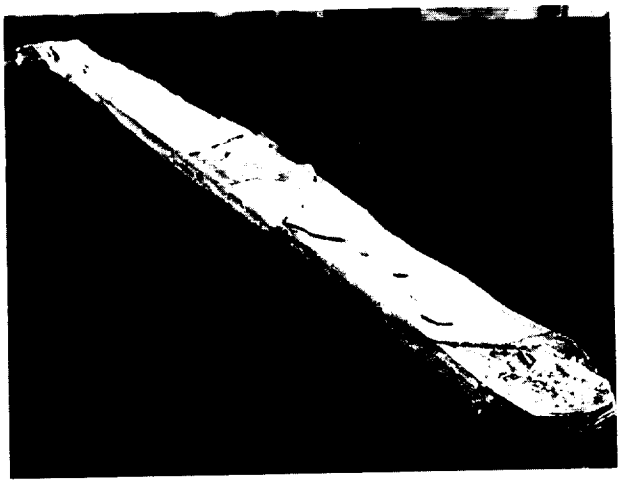

(a) Completion of spiral fold

(b) Evacuation setup

(c) Compaction of parachute

(d) Parachute in clam-shell

(e) Clam-shell in metal canister

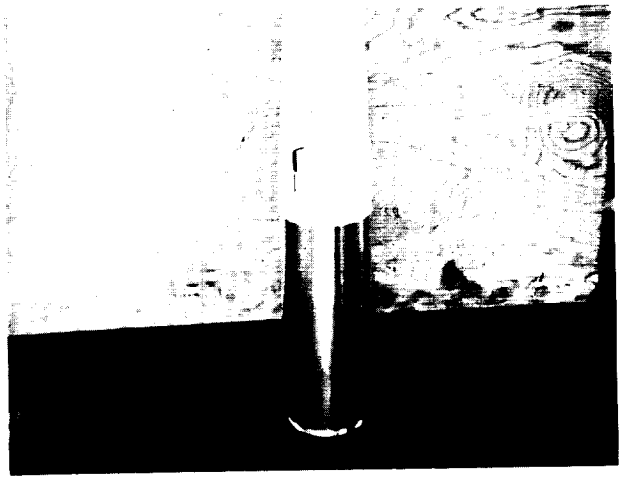

(f) Packaged configuration

Figure C-2. Reduction of Package Size and Installation of Parachute in Canister

APPENDIX D

JUNE, 1972, WALLOPS ISLAND FLIGHT TESTS OF THE STOKES-FLOW PARACHUTE

SUMMARY

An examination of the performance and testing deficiencies of the 14 m^2 Stokes-flow parachute during the June, 1972, Wallops Island flight test is presented below. Although the performance expectations of the parachute desired by NASA personnel were not met due to partial brace collapse, all the occurrences during the tests were theoretically predictable. The parachute delivery system was subject to unacceptably large deployment loads (beyond previous design values) caused by excessively high horizontal apogee velocities at low injection altitudes. This particular parachute payload system was not designed for high loading deployments in conjunction with the standard Arcas meteorological rocket. However, design changes to improve its ultimate strength could be incorporated into future parachutes if low altitude deployments are necessary. Past systems discussions focused on apogee deployments above an altitude of 80 km using the RDT & E motor.

The third of the four rocket firings is examined in some detail because it had the largest parachute drag generation as a consequence of having the highest deployment apogee in the test series. Flight test L1-5482, designated as Test 3, achieved an apogee altitude of 74.17 km (243,266 ft) with parachute deployment close to this condition. The parachute's capability, a dynamic pressure of 0.750 N/m^2 , was exceeded. A flight test dynamic pressure of 0.957 to 1.480 N/m^2 caused a partial folding back of the braces. The loading in the other three tests far exceeded that of L1-5482 and the foldback streamer action was inevitable. Down to 36,600 m , Test 3 retained a semideployed state in which the braces were bent approximately 45 to 55 degrees back of the design (flat) condition. Substantial drag was generated even though there was a significant reduction in frontal area. The theoretical average drag coefficient, $C_{D_{Ao}} \approx 0.7$, was not achieved, but a drag coefficient of $C_{D_{Ao}} = 0.26$, was measured for an extended period of the test.

The parachute operational characteristics with the single payload suspension line do not allow a deceleration situation which exceeds the ultimate bending strength of the brace. Once the tubular structure is bent downwind into a post-buckled state, there is little chance that the structure will recover; rather,

the situation will become progressively worse as the parachute descends because of decreasing differential pressure in the brace tubes.

Evaluation from this flight data of several important vehicular and atmospheric characteristics is not feasible since correlation of theoretical estimates to experimental data is impossible. Similarly, the dynamic characteristics of the parachute cannot be correlated to the varying motions of the atmosphere -- turbulent fluctuations and wind movements. The latter correlation is important (especially with the future winddrifter flights), if spectral wind analysis is to be performed.

Considering the extremes imposed upon the decelerator, the following conclusions were drawn pertinent to Test 3:

1. None of the launchings had a chance for successful parachute descent due to the abnormal loading. A partially modified, payload-carrying parachute and winddrifter could be constructed to handle low altitude, high velocity deployments.
2. Substantial drag was generated despite the partially "feathered" state.
3. The parachute apparently deployed and inflated properly, probably confirming that the "double-pocket" inflation system operated properly.
4. The parachute operation can be matched by theoretical analysis.
5. The tubular structure retained integrity and positive strength, despite being loaded beyond its limits.
6. There is every indication that the parachutes tested are viable decelerators, and, with proper flight window insertion, would perform excellently. A sufficient amount of preflight engineering should be incorporated into each of these preliminary tests to prevent similar partial failures, and to ensure that the parachutes will perform so as to provide the valuable flight data that is needed.

DISCUSSION

The first field tests of the 14 m^2 X-brace Stokes-flow parachute were performed at Wallops Island, Virginia, during June 28-30, 1972, under the direction of NASA Langley Research Center. The parachute (decelerator) and instrumentation package were carried aloft in standard Arcas sounding rockets. Four launchings were made and in all cases parachute deployment occurred below 75 km . Radar tracking of each aluminized mylar parachute provides a complete record in standard Cartesian coordinates of its position as a function of time. Configuration identification and radar tracking data were sent to Astro Research for a one week preliminary evaluation in August, 1972. Detailed trajectory analysis is not included in this report because of minimal funding and, more importantly, because of the nature of the tests and their results.

The four launchings are designated as follows:

Test	Series	γ (degree)	Apogee (km)	Time (h,m,s)
1	L1-5480	~ 80	63.098	1825 Z
2	L1-5481	~ 80	69.664	1708 Z
3	L1-5482	~ 80	74.166	1841 Z
4	L1-5483	~ 80	70.250	1508 Z

The apogee altitudes of all but possibly Test 3, were too low, since the parachute was designed for deployment in the 80 to 90 km altitude range. Only Tests 2, 3, and 4 will be discussed and only Test 3 detailed. The higher apogee was desired for several reasons, including:

1. Critical altitude meteorological information.
2. Evaluation of extremely rarefied drag generation ability utilizing the Stokes-flow concept.
3. Low deployment and descent loading on the parachute.

The next section considers this last reason in further detail and indicates that at the lower altitudes of $H < 80$ km , there is a maximum acceptable vehicle and wind velocity condition at each

deployment altitude.

The following data was assumed common for the four flights.

$m_p = 0.175$ kg	payload attached by single center tie line
$m_c = 0.081$ kg	canopy mass
$m_b = 0.089$ kg	brace mass
$m_v = 0.014$ kg	inflation substance, n-pentane
$m_d = 0.195$ kg	total decelerator
$\epsilon = 0.190$	solidity of canopy material (mylar-nylon knit, type DD)
$d = 0.088$ m	brace diameter
$L = 5.300$ m	brace total length of mylar laminate, type Dow PZ-5508.36
$T_b \geq 250°$ k	internal brace temperature which generates a brace pressure of $P_b \geq 53$ mm Hg

Langley Research Center considered inflation substances other than n-pentane for these four parachutes, settling on Freon-113. The high molecular weight of Freon required that 40.4 gm be used in order to achieve gas pressures similar to those of n-pentane. Except for this, the above data were assumed to be correct.

Deployment near the apogee condition in a quiescent atmosphere occurred at the following dynamic pressures:

	Test 2	Test 3	Test 4
Dynamic Pressure (N/m^2)	2.24	0.92	6.85

Inclusion of headwinds (to 55 m/sec) and late or early deployment increase the dynamic pressure still further. As previously mentioned, these parachutes were designed for deployment in the

80 - 90 km range in order to avoid large loadings. These four payload-carrying parachutes were limited to an ultimate loading of 7.5×10^{-1} newtons/m^2 and less when normal safety margins are included. Thus, these three flights were all deployed significantly beyond design capability. Test 3 experienced the lowest deployment loads and resulted in the best flight data, and is the subject of a simplified trajectory analysis given later.

Detailed evaluation of parachute drag coefficients, particularly after apogee deployment, was not performed because of the poor delivery altitude. Normally, a three degree-of-freedom digital program correlating the rockets' ballistic trajectories and the horizontal winds to the parachute positions should be used to obtain the drag coefficient.

The characteristics of the parachute were derived by a simplified approach, assuming no lateral forces (lift). Calculation of the drag coefficient cannot be performed without some assumptions because of five unknowns:

$C_{D_{Ao}}$ = drag coefficient (directed opposite to the motion, relative to the air mass, of the parachute)

ρ = density

W_x, W_y, W_z = three wind velocities

There are three force equations, $\sum F_x = 0$, $\sum F_y = 0$, and $\sum F_z = 0$, which describe the motion. A general solution is usually obtained by making assumptions on two of the five unknowns. In our case, the trajectory was considered in several parts and assumptions were made on one wind component and density. The 1962 U.S. standard atmosphere was used in all calculations. Temporal density variations were not included. Vertical wind motions are believed to be relatively small during deployment, particularly in the altitude range of 40 - 70 km . During deployment at apogee the horizontal wind velocities are important especially if they were headwinds.

On the descending portion of the parachute trajectory, (below 70 km altitude), the horizontal wind components, W_x , and W_y , are important. The parachute velocity, v , relative to the air mass becomes:

$$v = \sqrt{(\dot{x} - W_x)^2 + (\dot{y} - W_y)^2 + \dot{z}^2} \qquad (1)$$

Equilibrium of forces results in the expression:

$$\tfrac{1}{2}\,\rho\, C_{D_{Ao}}\, A\, v\, \vec{v} + m(\bar{a} - \bar{g}) = 0$$

where $\vec{v}$ is the parachute relative directed velocity, and $\bar{a}$ is the acceleration. The drag coefficient is:

$$C_{D_{Ao}} = -2m\,(\ddot{z} - g)/\,\rho A v\,\dot{z} \qquad (2)$$

In component form the wind velocities are:

$$W_x = \dot{x} + 2\,ma_x/C_D\,A\rho v$$

$$W_y = \dot{y} + 2\,ma_y/C_D\,A\rho v$$

$$W_z \equiv 0$$

Eliminating the density from the wind calculations results in:

$$W_x = v_x - (\ddot{x}\,\dot{z})/(\ddot{z} - g)$$

$$W_y = v_y - (\ddot{y}\,\dot{z})/(\ddot{z} - g)$$

From the previous expressions it is shown that the assumption of zero lift allows the calculation of winds directly from radar tracks. In the third section of this appendix, Recommendations/Future Applications, several important assets of the parachute are discussed relative to lift and response rates.

An evaluation of drag and dynamic pressures, $\tfrac{1}{2}\rho\, v^2$, for Test 3 is now in order. Figure D-1 indicates the trajectory, drag coefficient, and dynamic pressure using equations (1) and (2) for altitudes below 70 km. Because of the brace collapse, the parachute descent rate was quite rapid and high frequency

winds were not discernable. The prevailing winds for altitudes of $H > 45$ km caused a near constant drift in which $\dot{x} - W_x = 0$, and $\dot{y} - W_y = 0$. Between 70 and 74 km, the wind characteristics are difficult to estimate without recourse to trajectory matchings. However, a fairly complete picture can still be patched together. Figure D-1 indicates that from deployment and through descent to $H \approx 37$ km, a significant drag coefficient was generated. The nominal expectations, $C_{D_{Ao}} \approx 0.7$, were not realized and it is estimated that the parachute retained a 45° brace bend as indicated in the following sketch:

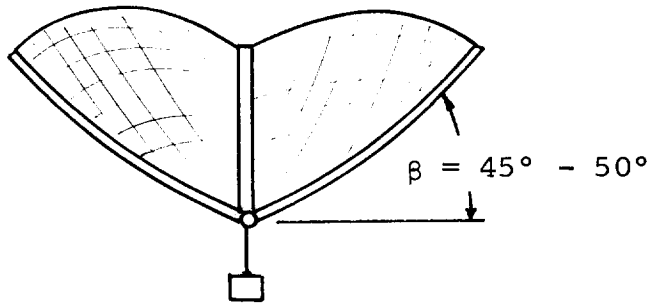

It is possible for the braces to reach an equilibrium position in the folded-back position of $\beta < 90°$, because the restoring moment that the braces exert increases as β increases.

The parachute performance data (see Figure D-1) shows that the dynamic pressure remained approximately constant during the descent to 35 km. Accordingly, the brace folded-back angle would have to remain approximately constant during that part of the descent. For it to remain so appears to be plausible inasmuch as the ambient pressure increases only slightly in that period. Thus, the inflation pressure in the braces and their restoring moment would have also remained approximately constant.

The data in Figure D-1 indicates a large increase in dynamic

pressure at an altitude of 35 km . It is surmised that the braces folded back to 90° at that point and remained so for the rest of the descent. It is conjectured that a wind condition and/or a low differential pressure on the braces at this altitude induced the complete streamer action. The remainder of the flight is not important, as the drag coefficient decreased an order of magnitude (compared to earlier values), while the dynamic pressure increased an order of magnitude.

FLIGHT TEST GUIDELINES

The critical phase of the parachute operation occurs during the time beginning with the initial deployment of the spiral-packaged parachute from the rocket payload canister, and ending with the subsequent inflation and stiffening of the structural braces. The X-brace structure must be deployed during the short time span in which it is still subject to minimal aerodynamic loads. Failure to meet such criteria will result in the loss of load-carrying capability due to either brace rupture or post-buckling of this tubular structure. The latter type of parachute failure (without payload) was shown from drop tests in Figure 40 of Reference 5. By exceeding the maximum moment capability at the center intersection, the braces fold aft decreasing the drag area and increasing the terminal velocity.

Acceptable time spans for fluid injection into the braces and altitude insertion requirements are given in References 6 and 7 respectively, and are repeated as follows. The maximum allowable rate of fluid ejection by the pockets during deployment of the full scale parachute was determined by relating deployment pressure to deployment rate. The analysis led to this general equation:

$$t = 0.324 \sqrt{\frac{m_t \, L}{p \, r^2}}$$

where

r = brace tube radius

p = deployment pressure

m_t = total parachute mass

L = brace tube half-length

t = minimum time for full deployment

If full scale parameters ($r = 0.04$ m , $p = 5$ mm Hg , $m_t = 0.186$ kg , $L = 2.67$ m) are used, the minimum deployment time is 0.22 second . A total time of 2.5 seconds is required for fluid emission from the pockets so that the pressure remains at a minimal 5 mm Hg during deployment, and increases to

75 mm Hg at full pressurization.

The fluid pockets are designed so that during deployment the fluid is forced out of a small hole or holes by the fluid vapor pressure. The dynamic pressure of the escaping fluid is assumed equal to the vapor pressure of the liquid; $\frac{1}{2}\rho v^2 = p$. The rate of loss of fluid mass is $\dot{m} = \rho v A$. The time, t, for full expulsion of fluid of mass, m, density, ρ, and vapor pressure, p, through holes of total area, A, and orifice factor, K, is then

$$t = \frac{K m}{\sqrt{2\rho p}\, A}$$

To achieve the desired mass flow in a 2.5 second time period, the hole size should be 0.022 in. in diameter when using n-pentane at an initial temperature of 288°K. Different flow rates can be calculated using the previous expression. The four pockets used in the X-brace parachute are located near the ends of each brace. The braces should be inflated during the minimal time period in which rupture will not occur. Extended deployment times, (e.g., $t > 2$ sec), at low altitudes could result in positive inflation, but only of a post-buckled structure that will not recover into the flat X-brace orientation necessary to **hold out the drag-producing mesh.**

The parachute is subject to large loads during deployment, deceleration descent from high altitudes, and during descent in a gusty, windy or turbulent atmosphere. The parachute has been designed to withstand a 1.6 g-loading while carrying a meteorological data package. The g-loading capability of this configuration depends upon the brace ultimate bending strength. The structural characteristics of inflated tubular members have been discussed in Reference 5, and the structural moment was given by the relation $M_\sigma = K\pi P r^3$, where

P = internal tube pressure

r = tube radius

K = buckling correlation factor typically varying from 0.6 to 1.0 ($K = 1$ for a total collapse load)

At the brace intersection in an equilibrium descent condition, M_σ must react to the force bending moment, M_c , due to aerodynamic and structural loads. Loads on the parachute are indicated in the following sketch,

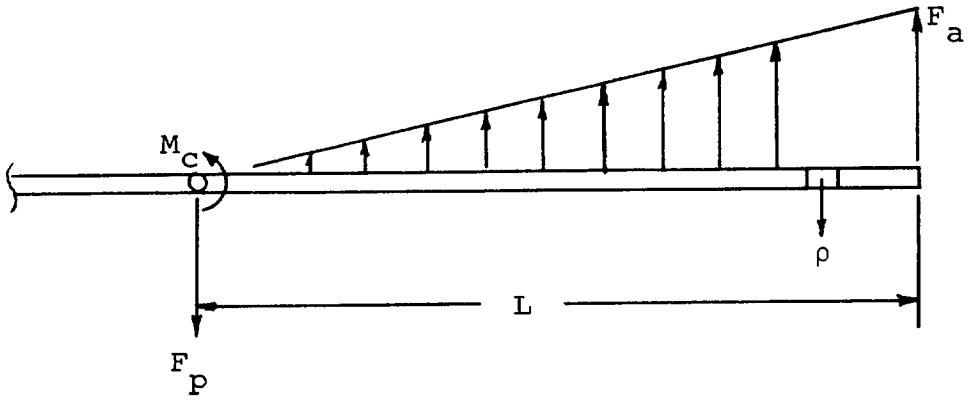

where

M_c = hub loading moment

$F_p = m_p a$, payload force

m_p = payload mass

a = parachute acceleration

ρ = mass/length of brace and canopy

F_a = force/length generated by Stokes-flow aerodynamics

m_b = mass of brace

m_{bc} = mass of brace and canopy

Define the parameter as $x = m_p/m_{bc}$. Through statics one obtains the hub moment:

$$M_c = \left(\frac{\frac{m_b}{m_{bc}} + 4x}{24} \right) m_{bc} \; a \; L \qquad (3)$$

For the flight test vehicle, the hub moment becomes:

$$M_c = 0.2 \; m_{bc} \; a \; L$$

The calculations of various critical parameters can now be made by equating the force bending moment, M_c , with the ultimate structural bending strength, M_σ . For example, the critical internal pressure needed to retain integrity is:

$$P_{crit.} \geq 0.2 \frac{m_{bc} \; L \; g}{K\pi \; r^3} \; n_g$$

where

g = acceleration of gravity

$n_g = a/g$

Substituting the proper numbers for the flight test parachute, one obtains:

$$P_{crit.} \left[\text{mm Hg} \right] \geq 28.1 \; n_g$$

Thus, for $n_g = 1.6$ (g's) a minimal internal pressure of 45 mm Hg is required. The minimum required tube pressure, $P_{crit.}$, was presented in Reference 7 for a particular "flight envelope" situation, and is also presented in Figure D-2 for convenience.

The following conditions were assumed in order to obtain the results. The parachute was deployed at apogee with a velocity, $V_H = 150$ m/sec , which included any wind component. After deployment the parachute drag coefficient, $C_{D_{AO}}$, equaled 0.65 . For apogees of $H > 75$ km , the free-falling configuration accelerated to velocities greater than V_H . Reentering the "sensible" atmosphere at larger than deployment velocities, the vehicle experienced its greatest deceleration

loads. The minimum required tube pressure and g-loading for this parachute was realized by apogee deployment at $H \sim 75$ km . At lower altitudes the loading increased extremely rapidly due to the higher air density and dynamic pressure. Below 70 km the required tube pressure exceeded the dynamic burst strength of the brace material. An upper limit of 77 mm Hg brace pressure is indicated by line ③ of Figure D-2. This burst strength limit was obtained after investigating tube dynamic response, and represents a material ultimate yield stress of one-fifth the static value. Since variations in the brace properties, air density, etc., are possible, the critical brace loading was designated as 25% below the ultimate.

Flight windows for various apogee velocities are presented in Figure D-3, together with flight data points from Tests 2, 3, and 4. These test points are all outside the proper limits for low altitude deployment. The figure shows ultimate deployment capability (i.e., no structural safety factor).

RECOMMENDATIONS/FUTURE APPLICATIONS

The Stokes-flow parachute and winddrifter have a potential for becoming the "workhorse" meteorological tools of environmental analysis, particularly for measurements in the 30 - 90 km altitude band. The Stokes-flow parachute realizes a ballistic coefficient of:

$$\beta = 0.0377 - 0.0404 \text{ kg/m}^2 \quad (0.0077 - 0.0083 \text{ lb/ft}^2)$$

which includes a 175 gm payload. Subsonic descent below 83 km is possible. The winddrifter, (a parachute without payload), with a ballistic coefficient of:

$$\beta = 0.0194 - 0.0230 \text{ kg/m}^2 \quad (0.0039 - 0.0047 \text{ lb/ft}^2)$$

achieves subsonic descent when released from altitudes below 86 km . A simplified supersonic aerodynamic analysis in Reference 8 indicates the potential use of the Stokes-flow parachute at significantly higher altitudes. Figure 4, obtained from Reference 8, is included and indicates a drag coefficient of $C_D = 0.2$ to 0.8 at 70 and 90 km altitudes during supersonic descent. Apogee altitudes above 100 km can be foreseen as expanding the use of the parachute to include additional meteorological rockets, e.g., Super Loki Dart, Cajun Dart, Sidewinder Arcas, Boosted Arcas, etc. Higher altitude deployment will require that one or several modifications be chosen to increase the maximum loading capability of the parachute. Direct modifications include:

- Increasing the tube pressure to a maximum of 75 mm Hg .
- Increasing the tube pressure beyond the 75 mm Hg level by better control of the dynamic deployment rate.
- Increasing the tube pressure by using an inflation substance with a higher vapor pressure.
- Tapering the tubes and increasing the tube diameter while retaining a high vapor pressure.
- Using triangular gores (or, less reliably, using multiple suspension lines) to improve the structural load-carrying capability.
- Shifting the aerodynamic center of pressure inward by changing the mesh shape, while modifying the positions of attachment.

With one or several of the previous alterations, an increase in g-loading from $n_g = 1.6$ to $n_g = 2.3$ would allow deployments of the payload-carrying parachute at altitudes of up to 110 km . Using equation (3) , it can be seen that the hub moment of the payload-carrying parachute is nine times greater than that of the winddrifter. An internal brace pressure of the winddrifter can be nine times smaller than that of the payload parachute, and it will withstand the same maximum loading. It should be evident that the tests of the winddrifter would be significantly less crucial than the payload-carrying descents of the Stokes-flow parachute. The very low and very high altitude tests should first be performed with the winddrifter. The higher altitude winddrifter deployments at $H \geq 110$ km are definitely within the realm of possibility. Such deployments would descend at significantly lower velocities than would the Robin sphere. Wind response above 80 km could be obtained.

The Stokes-flow X-brace parachute's wind response below 80 km has been presented (assuming a non-lifting parachute) in Reference 6. Figure 5 obtained from this reference indicates very good correlation by following the first wind cycle below 80 km . The Starute does not match capabilities until nearly 20 km lower in altitude than the winddrifter. A rather simple time constant, t_c , as derived in Reference 16, has often been used to correlate non-lifting vehicle wind response. From Reference 16 one obtains:

$$t_c = \frac{2\beta}{\rho \dot{z}} \sim \dot{z}/g$$

where

$$\beta = \frac{M}{C_D A} \text{ , ballistic coefficient}$$

ρ = air density

$\dot{z}$ = vertical descent velocity

g = acceleration of gravity

The time constant, t_c , indicates the period for a 1/e (1/2.73) reduction in relative horizontal wind because the vehicle will begin to drift with this air mass. The change in altitude associated with this time constant is:

$$\Delta z_c = \dot{z} t_c = \dot{z}^2/g$$

The best wind response of drag devices thus requires lower descent rates, i.e., very low ballistic coefficients. Because of the partial "streamer-action" and higher descent rate of Test 3, the following height and time constants are larger than desired.

Time (sec)	Altitude (km)	V_z (m/s)	t_c (sec)	Δz_c (m)
160	72.71	132	13.50	1780
180	69.63	155	15.80	2450
240	62.56	92	9.40	865
840	36.94	25	2.55	64

Astro Research has designed a decelerator system which realizes an extremely low ballistic coefficient, and which will be inexpensive when mass produced. The hardware development program is nearly completed. However, immediate utilization of the winddrifter without an appraisal of its dynamic response can lead to erroneous evaluation of the flight data. The parachute and winddrifter are known to generate normal forces (lift and moments) that change the wind response rate of the configuration. The dynamic overshoot or undershoot must be filtered out of the data from configuration radar trackings if true spectral data are to be known. Similarly, keel type additions and billow angles could be specified to obtain a decelerator that will not generate a lift component during nominal angular shifts (i.e., $\alpha \approx \pm 20°$). There is also the possibility that lift response characteristics are advantageous since they emphasize, by over-responding, the high-frequency wind currents which are otherwise hard to measure.

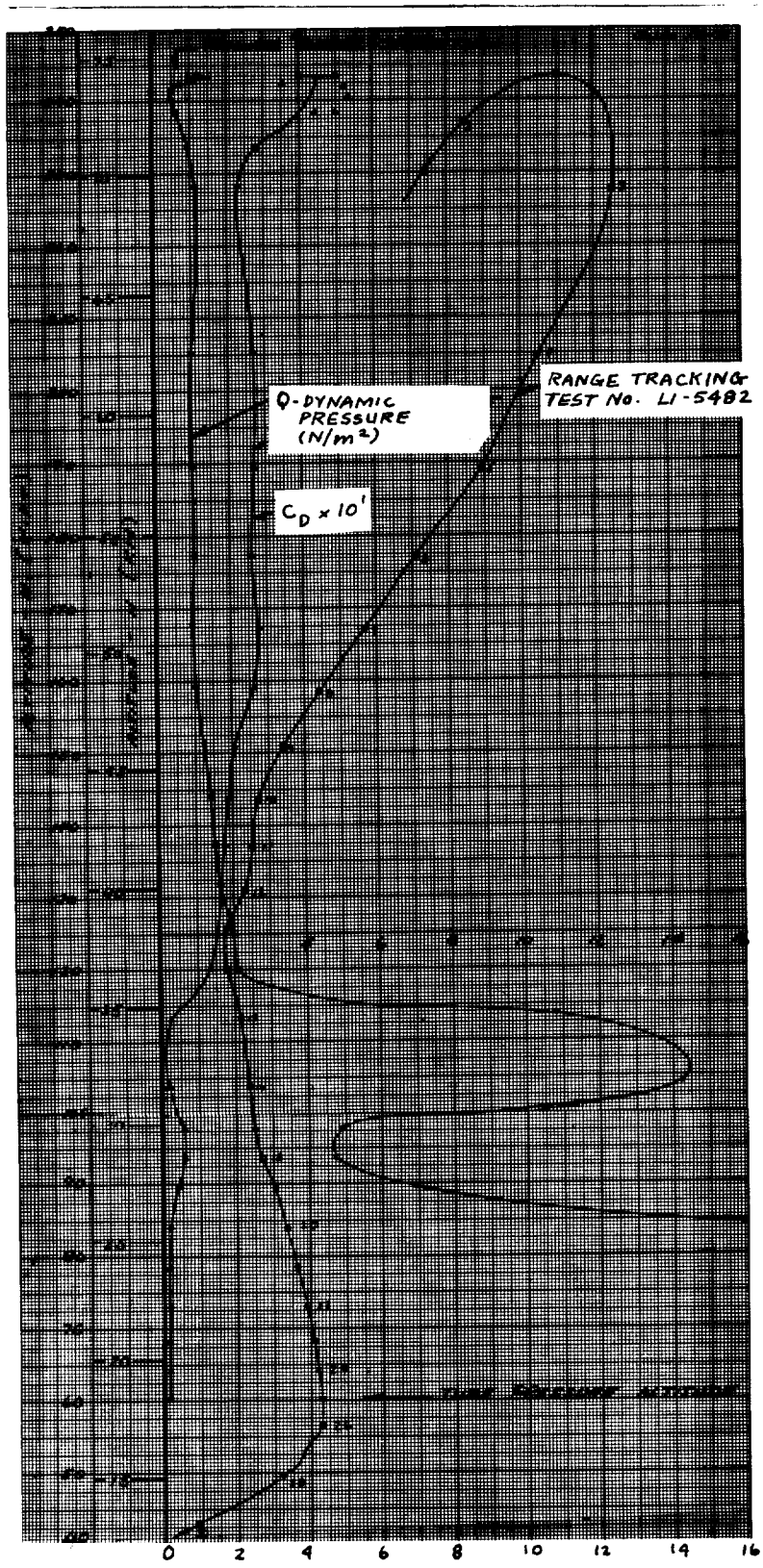

Figure D-1. Parachute Performance of Test No. 3 (L1-5482)

(1) LOAD = Brace Ultimate Bending Strength

(2) LOAD = 4/5 Brace Ultimate Bending Strength
(Minimum Recommended Design)

(3) Limit With Pressure = Burst Strength Of Brace

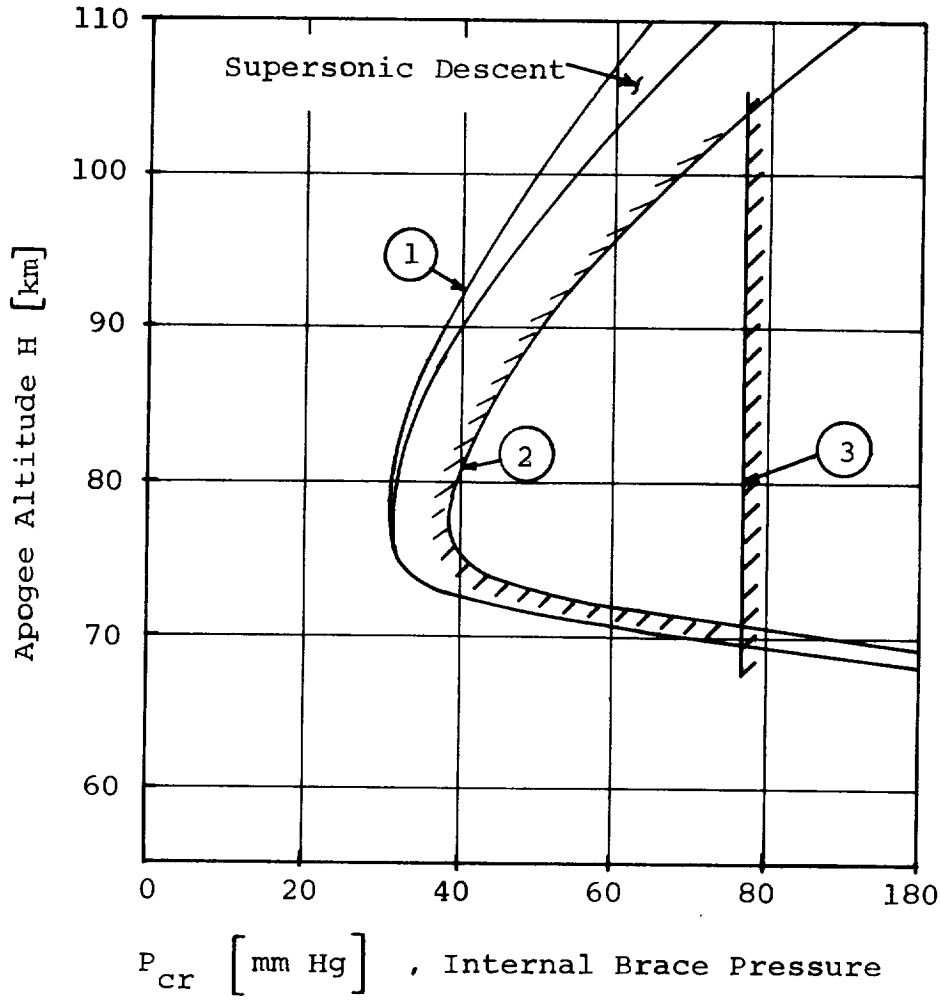

Figure D-2. Required Tube Pressure For 14 m^2 Stokes-Flow Parachute

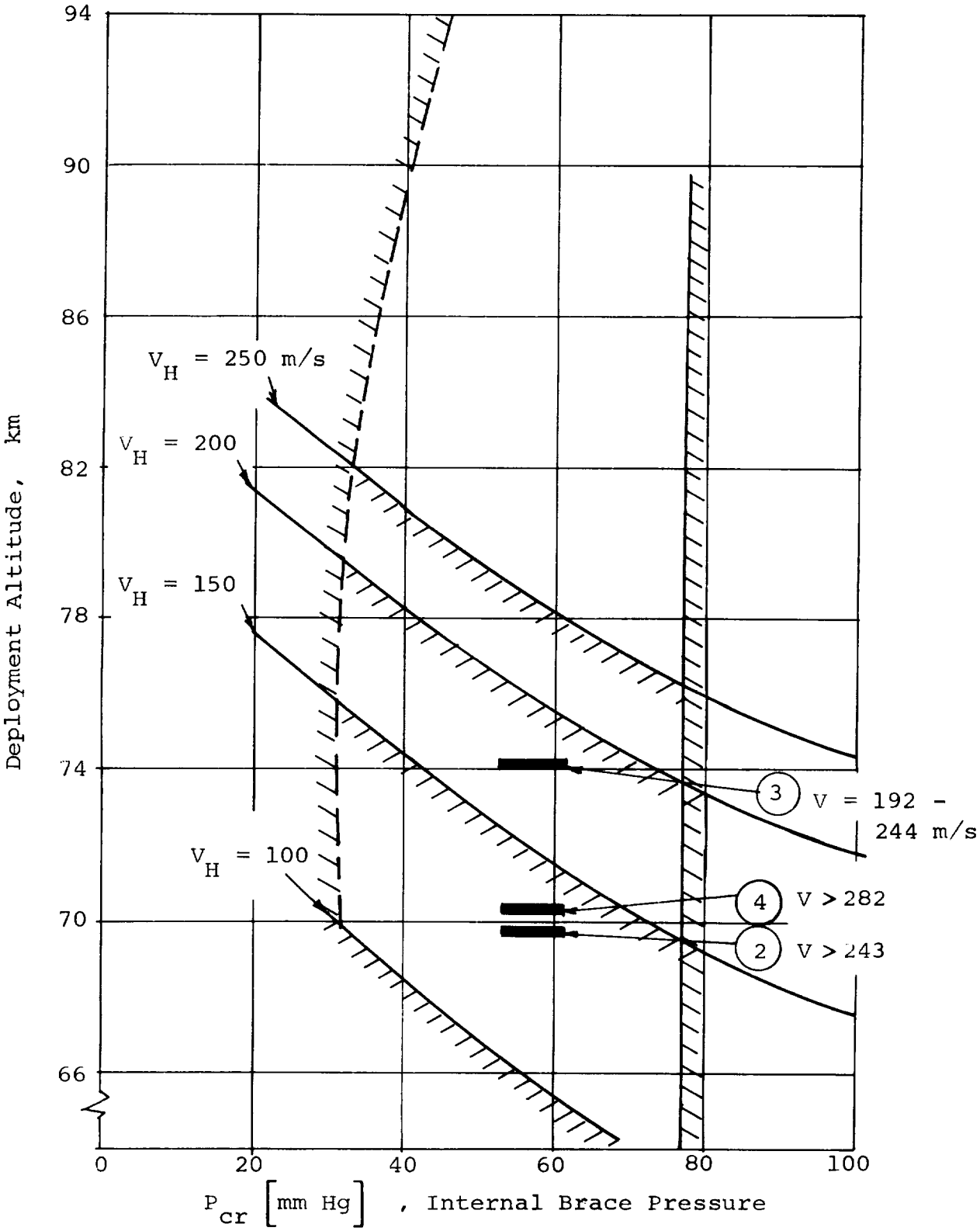

Figure D-3. Ultimate Deployment Capability of 14 m^2 Stokes-Flow Parachute With Payload

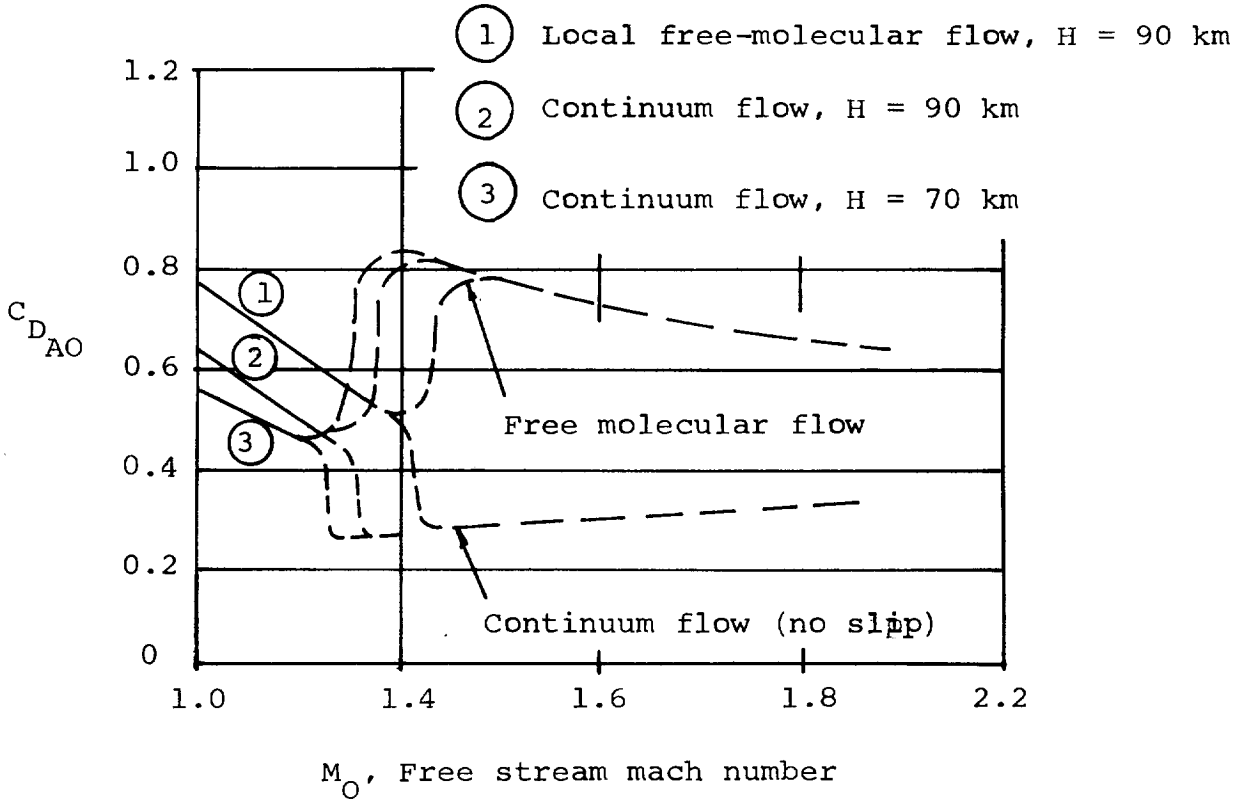

Figure D-4. Supersonic Flow of the Stokes-Flow Parachute, Solidity $\epsilon = 0.2$

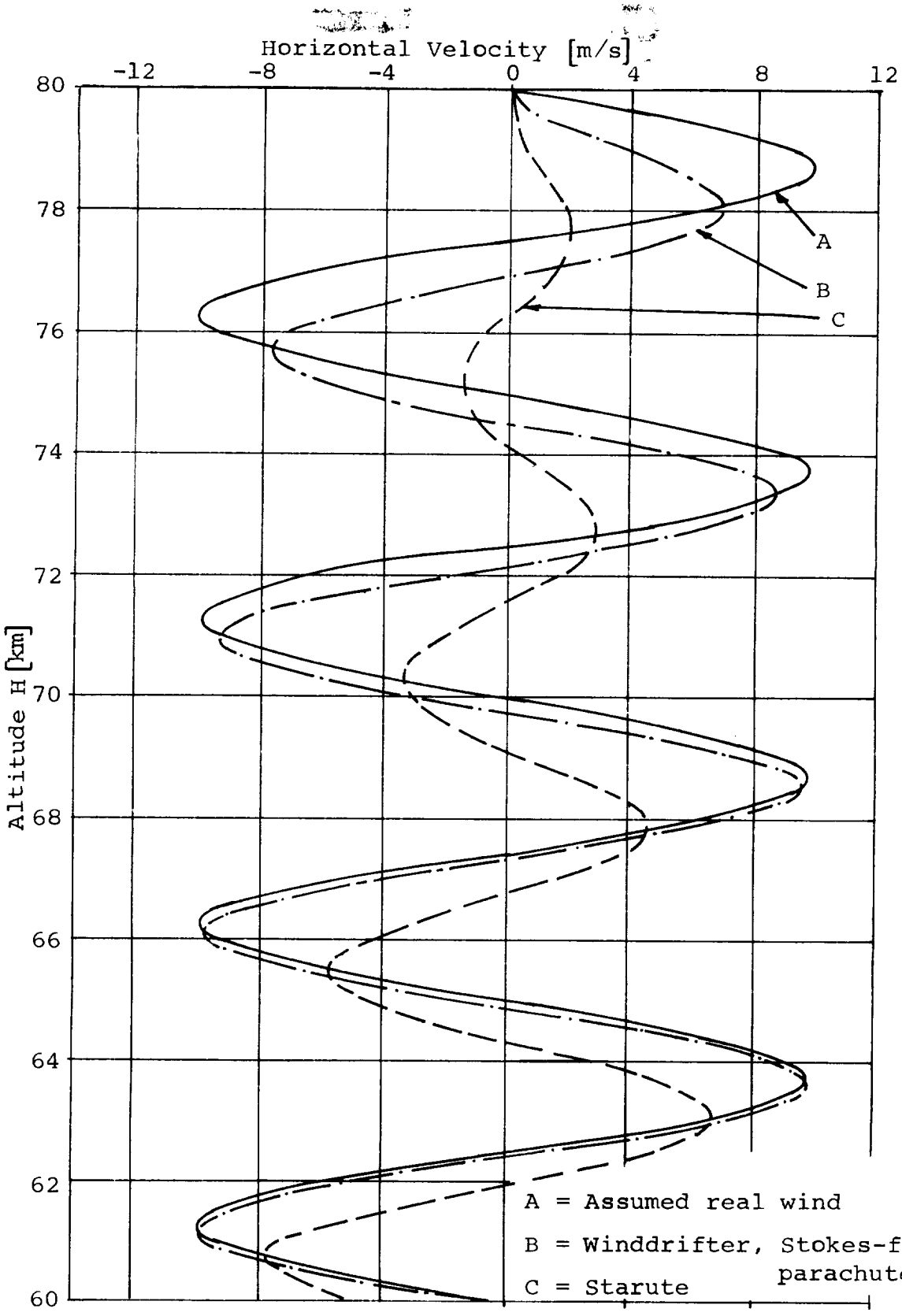

Figure D-5. Averaged Horizontal Velocity Response of Parachutes Vs. Descent Altitude

REFERENCES

1. U. S. Patent No. 3 386 692

2. Niederer, P.G.: Development of a High-Altitude Decelerator, Final Report on Contract NAS1-7770, NASA CR-66755, January 1969.

3. Niederer, P.G.: Development of an Extremely Lightweight High-Altitude Decelerator, AIAA Journal of Spacecraft and Rockets, Vol. 6, No. 11, 1969, pp 1274-1278.

4. Niederer, P.G.: Structural Considerations in the Development of Extremely Lightweight Decelerators, AIAA Paper No. 71-401 presented at the AAS/AIAA Variable Geometry and Expandable Structures Conference, Anaheim, Calif., April 21-23, 1971.

5. Niederer, P.G., Lewis, W.F., and Adams, L.R.: Development of a Stokes-Flow Decelerator for High-Altitude Meteorological Rocket Applications, Final Report on Contract NAS1-9881, Astro Research Corporation, ARC-R-513, December 1971.

6. Ground and Flight Test Program of a Stokes-Flow Parachute, Bi-Monthly Progress Letter No. 2, Contract NAS1-10947, November 1, 1971.

7. Letter to Mr. Erskine White from D.J. Mihora of Astro Research Corporation pertinent to "Flight Test Program", June 15, 1972.

8. Ground and Flight Test Program of a Stokes-Flow Parachute, Bi-Monthly Progress Letter No. 1, Contract NAS1-10947, September 3, 1971.

9. Fichtl, G.H.: Spherical Balloon Response to Three Dimensional Time-Dependent Flows, NASA TN D-6829, July 1972.

10. Luers, J., and MacArthur, C.: Ultimate Wind Sensing Capabilities of the Jimsphere and Other Rising Balloon Systems, NASA CR-2048, June 1972.

11. Adelfang, S.I., and Cocrit, A.: Jimsphere Wind and Turbulence Exceedance Statistics, NASA CR-2118, August 1972.

12. Pchelka, I., Petrenka, N., and Buldovsky, G.: Meteorological Flight Conditions for Supersonic Aircraft, NASA TT-F693, July 1972.

13. Stengel, R.F.: Wind Profile Measurement Using Lifting Sensors, Journal of Spacecraft, Vol. III, No. 3, March 1966.

14. Mahoney, J., and Boer, G.J.: Horizontal and Vertical Scales of Winds in the 30-60 Kilometer Region, Proceedings of the Third National Conference on Aerospace Meteorology, May 6-7, 1968.

15. Engler and Nicholas: Development of Methods to Determine Winds, Density, Pressure and Temperature from the ROBIN Falling Balloon, ARCRL Kept Contract AF 19 (604) - 7450, or ARCRL-65-448 (DDC - A D 630200).

16. Peterson, J.W., and McWalters, K.D.: The Measurement of Upper Air Density and Temperature by Two Radar-Tracked Falling Spheres, NASA CR-29, April 1964.